(2)

AD_____

Molecular Basis of Paralytic Neurotoxin Action on Voltage-Sensitive Sodium Channels

Annual/Final Report

William A. Catterall

October 20, 1989

Supported by

U.S. ARMY MEDICAL RESEARCH AND DEVELOPMENT COMMAND
Fort Detrick, Frederick, Maryland 21701-5012

Contract No. DAMD17-84-C-4130

University of Washington
Seattle, Washington 98195

SECURITY CLASSIFICATION OF THIS PAGE

REPORT DOCUMENTATION PAGE

Form Approved
OMB No 0704 0188
Exp Date Jun 30 1986

1a REPORT SECURITY CLASSIFICATION Unclassified	1b RESTRICTIVE MARKINGS
2a SECURITY CLASSIFICATION AUTHORITY	3 DISTRIBUTION / AVAILABILITY OF REPORT Approved for public release; distribution unlimited
2b DECLASSIFICATION / DOWNGRADING SCHEDULE	
4 PERFORMING ORGANIZATION REPORT NUMBER(S)	5 MONITORING ORGANIZATION REPORT NUMBER(S)
6a NAME OF PERFORMING ORGANIZATION University of Washington 6b OFFICE SYMBOL (If applicable)	7a NAME OF MONITORING ORGANIZATION
6c ADDRESS (City, State, and ZIP Code) Seattle, Washington 98195	7b ADDRESS (City, State, and ZIP Code)
8a NAME OF FUNDING / SPONSORING ORGANIZATION U.S. Army Medical Research & Development Command 8b OFFICE SYMBOL (If applicable)	9 PROCUREMENT INSTRUMENT IDENTIFICATION NUMBER DAMD17-84-C-4130
8c. ADDRESS (City, State, and ZIP Code) Fort Detrick, Frederick, MD 21701-5012	10 SOURCE OF FUNDING NUMBERS PROGRAM ELEMENT NO. 61102A; PROJECT NO 3M161. 102BS12; TASK NO AA; WORK UNIT ACCESSION NO 111

11. TITLE (Include Security Classification)
(U) Molecular Basis of Paralytic Neurotoxin Action on Voltage-Sensitive Sodium Channels

12. PERSONAL AUTHOR(S)
William A. Catterall

13a. TYPE OF REPORT	13b. TIME COVERED	14 DATE OF REPORT (Year, Month, Day)	15. PAGE COUNT
Annual/Final Report	FROM 9/15/84 TO 9/14/89	1989, October 20	42

16. SUPPLEMENTARY NOTATION
The Annual Report period covers 9/15/88-9-14/89.

17 COSATI CODES		
FIELD	GROUP	SUB-GROUP
06	01	
06	15	

18. SUBJECT TERMS (Continue on reverse if necessary and identify by block number)
Ion transport, sodium channels, action potentials, electrical excitability, neurotoxins, RA 1

19 ABSTRACT (Continue on reverse if necessary and identify by block number)

In years 1 - 5 of this project, progress was made on several objectives:

A. The sites and mechanisms of action on the sodium channel were examined and further defined for three new classes of neurotoxins: Goniopora toxins, Brevetoxins, and Conotoxins.

B. Monoclonal antibodies with high affinity for the mammalian neuronal sodium channel were developed and methods to screen them for activity at neurotoxin binding sites were established.

C. Site-directed antibodies against defined regions of the amino acid sequence of the sodium channel were prepared and shown to bind at discrete negatively charged subsites on the extracellular surface of the channel that may form part of neurotoxin receptor sites.

20 DISTRIBUTION / AVAILABILITY OF ABSTRACT ☒ UNCLASSIFIED/UNLIMITED ☐ SAME AS RPT ☐ DTIC USERS	21 ABSTRACT SECURITY CLASSIFICATION Unclassified
22a NAME OF RESPONSIBLE INDIVIDUAL Mary Frances Bostian	22b TELEPHONE (Include Area Code) 301-663-7325 22c OFFICE SYMBOL SGRD-RMI-S

DD FORM 1473, 84 MAR 83 APR edition may be used until exhausted
All other editions are obsolete

SECURITY CLASSIFICATION OF THIS PAGE

TABLE OF CONTENTS

Foreword

In conducting research described in this report, the investigator(s) adhered to the "Guide for the Care and Use of Laboratory Animals," prepared by the Committee on Care and Use of Laboratory Animals of the Institute of Laboratory Animal Resources. National Research Council (DHEW Publication No. (NIH) 86-23, Revised 1985).

RESEARCH REPORT

SUMMARY

In the past year we have made important progress on four aspects of our work toward defining the sites and mechanisms of both protein and low molecular weight toxins on sodium channels and toward development of antibodies which block toxin binding and action.

I. Actions of Neurotoxins on Sodium Channel α Subunits Transfected in Mammalian Somatic Cells. In order to determine definitively which functional neurotoxin receptor sites are located entirely on the α subunits, cDNAs encoding α subunits were expressed in Chinese hamster ovary cells. The α subunits were fully functional when expressed in these cells. Tetrodotoxin blocked these expressed sodium channels by binding at neurotoxin receptor site 1, veratridine persistently activated them by binding at neurotoxin receptor site 2, and scorpion toxin slowed their inactivation by binding at neurotoxin receptor site 3. These results show that all three of these receptor sites are located on α subunits.

II. Physiological Effects of Site-Directed Antibodies. Identification of an Inactivation Gating Segment. We have developed a panel of site-directed antibodies in order to identify toxin receptor sites on the sodium channel and to explore relevant antigenic regions for block of toxin binding. It has been of interest to examine the physiological effects of these antibodies to identify functionally important regions of sodium channels and to determine which antibodies may have toxic actions of their own. Several antibodies directed against intracellular domains were tested in single channel recording with brain neurons. Only Ab_{SP19} directed against the intracellular segment between domains III and IV blocks sodium channel inactivation. The characteristics of block of inactivation suggest that this segment serves as the inactivation gate of the sodium channel.

III. A Major Immunogenic Region near the Receptor Site for α-Scorpion Toxins. Analysis of the ability of synthetic peptides representing different segments of the sodium channel structure to block binding of monoclonal antibodies to the channel shows that all five monoclonal antibodies raised against purified sodium channels recognize peptide segments between transmembrane helices S5 and S6 in domain I near the site of covalent attachment of scorpion toxin derivatives to sodium channels. These results suggested that monoclonal antibodies might be effective inhibitors of α-scorpion toxin binding.

IV. Inhibition of α-Scorpion Toxin Binding by Antibodies. Site-directed antipeptide antibodies directed against residues 382-400 and 355-371 of the sodium channel α subunit inhibit α-scorpion toxin binding up to 60% in the range of 0.5 to 2 μM. Similar effects are observed with antibodies directed against residues 1676-1703, but not several other antibodies tested. These results suggest that segments in the extracellular region of domain I (residues 355-400) and domain IV (residues 1676-1703) interact to form the high affinity α-scorpion toxin receptor site of the sodium channel. Binding at this site is inhibited more effectively by the monoclonal antibodies described in section III above. These antibodies

inhibit binding nearly completely with half maximal inhibition at 0.4 to 1.3 μM. More potent antibodies against this region of the channel may be effective inhibitors of α-scorpion toxin action *in vivo*.

Current experiments ar directed toward identifying the structural features of the scorpion toxin receptor site at higher resolution and using methods similar to those described above to locate the receptor sites for additional protein and low molecular weight toxins which act on sodium channels.

I. Actions of Neurotoxins on Sodium Channel α Subunits Transfected in Mammalian Somatic Cells

Sodium channels mediate the major inward current responsible for the upstroke of the action potential in many excitable cells. Rat brain sodium channels are heterotrimeric proteins consisting of α, β_1 and β_2 subunits of 260 kDa, 36 kDa and 33 kDa respectively (Catterall, 1986; Catterall, 1988a; Catterall, 1988b). A wide variety of neurotoxins affect sodium channel activity and five different toxin receptor sites on the rat brain channel have been biochemically characterized (Catterall 1986; Catterall, 1988a; Catterall, 1988b). Three distinct subtypes of the rat brain sodium channel α subunit, R_I, R_{II} and R_{III}, have been cloned and sequenced (Noda et al, 1986a; Kayano, 1988). Expression of α subunits by injection of mRNA into *Xenopus* oocytes has shown that many sodium channel functions are mediated by the α subunit alone (Noda et al, 1986b; Suzuki et al, 1988; Goldin et al, 1986; Auld et al, 1988). However, high molecular weight brain mRNA or R_{IIA} mRNA direct the synthesis of sodium channels with unusually slow inactivation kinetics (Auld et al, 1988). Co-expression with size-fractionated brain mRNA smaller than 4 kb is able to accelerate inactivation, suggesting that a low molecular weight brain protein is necessary for rapid inactivation in oocytes (Auld et al, 1988). We have stably expressed cDNA for the R_{IIA} α subunit in Chinese hamster ovary (CHO) cells, a mammalian cell line that lacks endogenous voltage-sensitive sodium channels, in order to examine the physiological and pharmacological properties of these channels in the genetic background of a mammalian somatic cell.

CHO cells were co-transfected with pVA222 containing the coding region of the R_{IIA} sodium channel α subunit (Auld et al, 1988) in vector pECE (Ellis et al, 1986) and pSV2 NEO, a plasmid conferring resistance to the antibiotic G418. Control transfections with pECE lacking the α subunit were also performed. Transfectants were selected through multiple passages in the presence of G418. Seven independent stable G418 resistant cell lines were isolated and analyzed for the presence of the α subunit transcript using the RNase protection procedure. As shown in Figure 1A, pVA1 and pVA4 (lanes 5 and 8) expressed RNA which protected a 781 nucleotide cRNA antisense transcript covering nucleotides 50 to 831 of the R_{IIA} 5' region (Auld et al, 1988). Northern blots showed that these two cell lines expressed mRNA species of approximately 7.5 kb and 3.5 kb which were specifically recognized by a R_{IIA} cRNA probe (Fig. 1B, lanes 3 and 4). While 7.5 kb is the expected size for transcription of the R_{IIA} cDNA in the pECE vector, the 3.5 kb species is truncated, possibly due to premature termination of transcription or abnormal RNA splicing within the cDNA expression unit. Cell line CP1, which was transfected with vector only, did not have detectable levels of mRNA encoding sodium channels (Figure 1B, lane 2). In contrast to the transfected cells, rat brain neurons in primary cell culture express the full length α subunit mRNA of 9.0 kb (Fig. 1B, lane 1). Variation of the input RNA to give comparable hybridization signals indicated that α subunit mRNA was approximately 10% as abundant in transfected cells as in rat brain (not shown). The RNase protection experiments, which are sensitive to even single nucleotide differences, confirm that the mRNA expressed in these cells is transcribed from transfected R_{IIA} cDNA.

The expression of functional channels on the cell surface was assayed by whole cell voltage clamp (Hamill et al, 1986). Cells of the two α subunit-transfected cell lines, PVA1 and PVA4, generated inward currents that activated and then inactivated within 2 msec in response to depolarizing voltage steps of increasing size (Fig 1C). Control transfectants did not produce a similar voltage-activated inward current (CP1, Fig 1C, Table 1). Voltage-activated inward currents were observed in greater than 70% of the PVA1 and PVA4 cells (Table 1). The properties of these inward currents remained stable through more than 27 passages after transfection.

The voltage-activated inward currents in transfected cells were reversibly blocked by 80 % in the presence of 100 nM TTX (Fig. 1D) and completely blocked by 200 nM TTX (not shown, n=3). The presence of voltage-activated inward currents only in transfected cells, their inhibition by TTX, their rapidly inactivating time course, and their reversal potential near +70 mV indicated that these currents were mediated by sodium channels encoded by the transfected R_{IIA} cDNA clone.

The mean peak sodium current was approximately 150 pA in both PVA1 and PVA4 cells (Table I), corresponding to the simultaneous activation of approximately 140 sodium channels with a single channel conductance of 18 pS (Stühmer et al, 1987) per cell. Comparison with the cell capacitance indicates a current density of 9.0 pA/pF and a density of sodium channels that are active during the peak current of 0.1 per μm^2 of cell surface area. In contrast, similar estimates of the density of active sodium channels at peak current indicate that mouse neuroblastoma cells have a sodium channel density of approximately 2-20 channels per μm^2 (Moolenaar & Spector, 1978; Gonoi et al, 1984) and the cell bodies of rat central neurons have a channel density of 3-10 channels μm^2 (Sah et al, 1988; Huguenard et al, 1988; Coombs et al, 1988). Evidently, the expression of active sodium channels in these transfected cell lines is much lower than that achieved in neuronal cells.

The voltage-dependence of activation of the Na^+ currents is consistent with the properties of sodium channels encoded by the R_{IIA} α subunit cDNA. In average current-voltage (I-V) relationships for peak inward sodium current from PVA1 cells (Fig. 2A), inward sodium current is first evident near -20 mV and peak inward current is achieved between +10 and +20 mV. Activation curves derived from peak currents (Fig. 2B) have half activation voltages near 0 mV. The peak Na^+ current is activated at a voltage that is 10 to 20 mV more positive than peak sodium currents recorded under similar conditions in cultured embryonic rat brain neurons (Coombs et al, 1988), or in different recording solutions in acutely isolated brain neurons (Sah et al, 1988; Huguenard et al, 1988), and oocytes injected with brain poly A+ mRNA (Auld et al, 1988), R_{II} mRNA (Noda et al, 1986), or R_{III} mRNA (Suzuki et al, 1988). A similar voltage-dependence was observed in every PVA1 and PVA4 cell that was studied. As in CHO cells, injection of R_{IIA} α subunit mRNA into *Xenopus* oocytes yields sodium channels with peak currents at +10 to +20 mV (Auld et al, 1988). A relatively positive voltage-dependence of activation of sodium channels expressed in either oocytes or CHO cells appears to be a signature that distinguishes sodium channels encoded by this α subunit clone from other sodium channels that have been studied.

The decay of sodium currents during a sustained depolarization was rapid in PVA1 cells with a $\tau_{1/2}$ of 0.7 msec at +10 mV (Fig. 2C, solid line). Inactivation time constants in PVA1 cells were similarly rapid at all potentials tested (Fig 2D). Steady state inactivation of the sodium current had an unusually steep voltage-dependence in PVA1 cells (Fig. 2B, Table 1). There was virtually no resting inactivation at our normal holding potential of -67 mV, whereas depolarization to -50 mV resulted in half maximal steady state inactivation. The sodium channels were essentially completely inactivated by -30 mV, and little or no overlap of the activation and inactivation curves was observed (Fig. 2B). Steady state

sodium current resulting from such overlap has been reported in neurons and suggested to contribute to the generation of bursts of action potentials (Stafstrom et al, 1985). R_{IIA} sodium channels are unlikely to contribute significantly to this aspect of neuronal excitability.

The time course and voltage-dependence of inactivation of sodium currents resulting from expression of R_{IIA} sodium channels in CHO cells are comparable to those of sodium currents in embryonic brain neurons in cell culture (Coombs et al, 1988) or acutely dissociated adult central neurons (Sah, Gibb, & Cage, 1988; Huguenard, Hamill & Prince, 1988). In contrast, sodium currents resulting from expression of R_{IIA} in oocytes inactivate much more slowly (Auld et al, 1988). In Fig. 2C, sodium currents during a depolarization to +10 mV are compared for sodium channels expressed in PVA1 cells (solid trace) or in oocytes (dotted trace, Fig. 6D in reference Auld et al, 1988). In CHO cells, currents inactivated within 1-2 msec whereas, in oocytes, inactivation was incomplete by the end of a 16 msec pulse. Recovery from inactivation in CHO cells was also rapid since no decrease in peak currents was seen during trains of pulses applied at 5 Hz (not shown). Sodium currents in oocytes injected with only the R_{IIA} α subunit mRNA diminish when stimulated with a similar protocol (Goldin et al, 1988). In previous work (Auld et al, 1988), it was found that these slowly inactivating sodium currents in oocytes could be converted to currents with kinetics similar to those in CHO cells by coinjection of low molecular weight RNA (< 4 kb), indicating that a low molecular weight protein can act to make the oocyte environment equivalent to that of the CHO cell. Candidates for this low molecular protein include $\beta 1$ or $\beta 2$ subunits, whose function remains unknown, and modulatory proteins such as protein kinases or enzymes involved in other post translational modifications. Our results show that this low molecular weight protein that is necessary for rapid inactivation kinetics of R_{IIA} sodium channels in oocytes (Auld et al, 1988) must either be endogenous or unnecessary in the different environment of the CHO cell.

Sodium currents mediated by native sodium channels are blocked by tetrodotoxin and saxitoxin acting at neurotoxin receptor site 1, persistently activated by veratridine, batrachotoxin, and other lipid soluble toxins acting at neurotoxin receptor site 2, and markedly potentiated and prolonged by polypeptide α-scorpion toxins and sea anemone toxins acting at neurotoxin receptor site 3 (Catterall, 1986). In order to test whether functional receptor sites for these three classes of toxins are present on R_{IIA} α subunits, we examined the effect of representative toxins on sodium currents in transfected CHO cells. As shown in Fig. 1D, tetrodotoxin inhibits sodium currents in PVA1 and PVA4 cells. The 80 % inhibition observed at 100 nM is consistent with a K_D of 25 nM in close agreement with previous biochemical studies of brain sodium channels (Catterall, Morrow & Hartshorne, 1979).

Veratridine and related lipid-soluble neurotoxins which act at neurotoxin receptor site 2 preferentially bind to activated sodium channels and cause persistent activation (Ulbricht, 1969; Leibowitz et al, 1986; Sutro, 1986; Rando et al, 1986; Rando et al, 1989). Their action is enhanced by repetitive activation of sodium channels. The effect of veratridine on sodium currents recorded in PVA1 cells is illustrated in Fig. 3. Panel A shows superimposed current traces recorded during a train of 10 consecutive pulses to +20 mV, a protocol designed to give a progressive increase in the number of veratridine-modified channels. Veratridine causes a sustained component of inward sodium current which is not inactivated during the 16 msec test pulses. In addition, there is a pulse-by-pulse increase in the sustained inward current recorded upon return to the holding potential following each pulse (Fig. 3A, arrow). This current represents inward sodium movement through persistently activated sodium channels which is increased at the negative holding potential (-100 mV) in comparison to the test potential because of the greater electrical driving force for sodium influx.

Veratridine acts on native sodium channels by preventing inactivation and by shifting activation to more negative potentials ((Ulbricht, 1969; Leibowitz et al, 1986; Sutro, 1986; Rando et al, 1986; Rando et al, 1989). The combination of these effects prevents channel closing on repolarization and causes the sustained inward sodium current. We also found that the voltage-dependence of activation for veratridine-modified sodium channels expressed from R_{IIA} cDNA was shifted to more negative membrane potentials. A population of veratridine-modified channels was generated by 10 successive depolarizations as in Fig. 3A. Following each pulse train, a test pulse was applied to a variable test potential. The voltage-dependence of veratridine-modified sodium channels obtained in this way is strongly displaced in the negative direction in comparison to control (Fig. 3B) as has been reported previously for veratridine acting on native sodium channels (Leibowitz, 1969; Rando et al, 1989).

Polypeptide toxins from Old World scorpions, called α-scorpion toxins, remove or greatly slow sodium channel inactivation (Catterall, 1986; Catterall, 1988a; Catterall, 1988b; Gonoi et al, 1984; Kopenhofer & Schmidt, 1968; Wang & Strichartz, 1985; Kirsch et al, 1989). Purified α-toxin from the scorpion *Leiurus quinquestriatus* slows inactivation of R_{IIA} sodium channels expressed in CHO cells (Fig. 3C). The rapid inactivation of sodium currents at positive test potentials is most strikingly affected. The slowing of inactivation allows increased peak sodium currents to be attained at each test potential (Fig. 3C) and causes a shift of the voltage-dependence of sodium channel activation to more negative membrane potentials (Fig. 3D). These effects are consistent with the actions of α-scorpion toxin on other mammalian nerve cells (14, 28).

Our results show that only the α subunit of the sodium channel is necessary for expression of functional sodium channels in CHO cells. Sodium channels composed of this single subunit are inhibited by tetrodotoxin acting at neurotoxin receptor site 1 and persistently activated by veratridine acting a neurotoxin receptor site 2. Their inactivation is slowed by *Leiurus* α-scorpion toxin acting at neurotoxin receptor site 3. These results show that the R_{IIA} α subunit cDNA is sufficient to encode neurotoxin receptor sites 1 through 3 in functional form.

From covalent crosslinking studies, *Leiurus* toxin is known to bind to a site near the contact regions of the α and β1 subunits and to react with residues in both of these subunits while specifically bound (Catterall, 1986; Catterall, 1988a; Catterall, 1988b). The site of covalent attachment of *Leiurus* toxin to the α subunit has been localized to the major extracellular loop in homologous domain I of the α subunit (Tejedor & Catterall, 1988). The present study provides direct evidence that the functional receptor site for α-scorpion toxins is indeed located on the α-subunit confirming that the primary binding site for that toxin is on, not just near, the α subunit.

II. Physiological Effects of Site-Directed Antibodies. Identification of the Sodium Channel Inactivation Gate.

A major goal of the present research is to identify the toxin receptor sites on the sodium channel and to develop antibodies which block toxin binding. Toward this end, a panel of site-directed antibodies have been developed and used to identify functional sites on the sodium channel. As part of our analysis, we have tested these antibodies for functional effects. In a previous study reported last year (Vassilev et al, 1988), we found that a conserved intracellular segment between homologous domains III and IV of the α subunit slowed inactivation of macroscopic sodium currents (Vassilev et al, 1989). The rate of onset of this effect during exposure to antibody was substantially slowed at depolarized holding potentials at which sodium channels were inactivated. It was concluded that the peptide segment between domains III and IV of the α-subunit is directly

involved in rapid sodium channel inactivation during large depolarizations. To further elucidate the mechanism of action of this antibody and to screen additional antibodies for functional effects, we have studied their effects on single sodium channels in inside-out membrane patches excised from rat brain neurons in cell culture.

Patch Clamp Experiments. Single sodium channels were studied using the excised patch clamp method (Hamill et al, 1981) applied to rat brain neurons in cell culture. To minimize the quantities of affinity-purified antibodies used, we developed a hanging-drop configuration of the patch-clamp technique as described in detail elsewhere (Vassilev, submitted for publication). Briefly, membrane patches were formed on the tip of a pipet filled with extracellular solution and excised into a bath filled with the same solution. The pipette tip was lifted out of the bath and introduced immediately into a small drop hanging at the tip of an agar-bridge capillary. The drop and the capillary contained intracellular solution at 21-23^{0}C and were connected to a chamber containing a Ag/AgCl reference electrode. Decreases in drop diameter due to evaporation were monitored and compensated by addition of fresh intracellular solution. The voltage dependence of activation and inactivation of Na currents shifted in the negative direction during the first few min of recording and then remained stable for up to 2 hrs. After stabilization, control recordings were taken. The antibodies dissolved in small volumes (1 - 3 µl) of intracellular solution were then added to the hanging drop. The onset of the antibody effect usually occurred in several minutes depending upon the holding voltage, and recordings were continued for 20 to 120 min. Solutions contained (in mM): intracellular, 105 CsF, 40 CsCl, 10 NaF, 5 EGTA, 5 HEPES, adjusted to pH 7.2 with CsOH; extracellular, 150 NaCl, 1.5 $CaCl_2$, 1.0 $MgCl_2$, 5.0 glucose, 5.0 HEPES, adjusted to pH 7.4 with NaOH.

Data Acquisition and Analysis. Membrane currents in excised patches were measured using Ag/AgCl electrodes connected to a List L/M-EPC-7 patch-clamp amplifier and filtered at 3 kHz (3 db) prior to digitization. Pulses were generated and filtered currents were sampled on line at 20 to 50 µsec per point using programs based on the Fastlab system (Indec Systems, Sunnyvale). Partial compensation of leakage and capacity current was obtained using the internal amplifier circuitry. Further digital compensation was obtained by subtraction from the experimental records of exponentials fitted to blank traces or to scaled records from hyperpolarizing pulses (Yue et al, 1989).

Specificity of the antibody effect. The functional effects of six anti-peptide antibodies on single sodium channels were examined (Fig. 4). These antibodies were directed against segments of all five major predicted intracellular domains of the α subunit as well as the short predicted intracellular segment between transmembrane segments S4 and S5 of homologous domain IV (see Experimental Procedures). In all control traces, sodium channel openings are clustered near the onset of the depolarizing pulses (Fig. 4A). Openings after the first few msec of the pulses are very rare events. In contrast, single channel openings continue throughout the 25 msec depolarizations in the presence of Ab_{SP19} (Fig. 4B, SP19). In other experiments, sodium channels continue to open and close throughout 250 msec depolarizing pulses in the presence of Ab_{SP19} (not shown). These results indicate that Ab_{SP19} completely blocks the process of rapid sodium channel inactivation. As a result, ensemble average currents are dramatically prolonged (Fig. 4C, SP19). None of the other five antibodies tested caused repetitive openings of single sodium channels throughout the depolarizing pulses (Fig. 4B), and none had a marked effect on the time course of the ensemble average currents compared to controls (Fig. 4C). The striking effect of Ab_{SP19} on single sodium channel currents and the lack of effects of other antibodies that bind to different intracellular segments provide substantial evidence for our previous conclusion (Vassilev et al, 1988) that the peptide segment between domains III and IV of α-subunit containing the recognition site for Ab_{SP19} is specifically involved in sodium channel inactivation.

The number of channels recorded varied from patch to patch. Typically, 1 to 5 functional channels were observed and multiple, superimposed openings clustered at the onset of the depolarizing pulses were recorded (Fig. 4). Ab_{SP19} dramatically increased the probability of channel opening late in the depolarizing pulses regardless of the number of channels recorded in the patch. Since the number of late openings was always much greater than the apparent number of functional channels, we assume that these late openings represent re-openings of individual channels rather than openings of channels for the first time after a long latency.

Voltage dependence of Ab_{SP19} action. The onset of the effect of Ab_{SP19} on inactivation of sodium channels in muscle cells under whole cell voltage clamp was more rapid at negative holding potentials (Vassilev et al, 1988). The excised patch preparation allows examination of this effect with better time resolution because barriers to diffusion of the antibody to its site of action are reduced. Fig. 5 illustrates the dependence of the onset of the effect of Ab_{SP19} on the holding potential. At -140 mV, single channel traces and ensemble average currents show channel openings clustered at the beginning of 25 msec depolarizing pulses (Fig. 5A, left column). After further control recordings at a holding potential of -80 mV (not shown), Ab_{SP19} was added to the intracellular side of the membrane patch. No alterations in sodium channel inactivation were observed during a period of six minutes after adding the antibody while holding the membrane potential at -70 or -80 mV (Fig. 5A., middle column). Returning the holding potential to -140 mV caused modification of the inactivation kinetics within 50 sec, as evidenced by the long, late channel openings throughout the depolarizing pulses (Fig. 5A, right column). After the antibody effect has occurred at -140 mV, it is not reversed by depolarization to -80 mV.

In a similar experiment, several records were taken under control conditions at -140 mV (Fig. 5B, left column). Within 20 sec after addition of Ab_{SP19}, the appearance of late, prolonged channel openings indicated substantial inhibition of inactivation (Fig. 5B, right column). Thus, the onset of the effect of Ab_{SP19} depends strongly on the holding voltage. At -140 mV, where the sodium channels are not inactivated, Ab_{SP19} acts rapidly to inhibit the inactivation process; at -70 or -80 mV, where sodium channels are substantially inactivated (see below), Ab_{SP19} does not alter channel inactivation within several min.

These results indicate that the effect of Ab_{SP19} on sodium channel inactivation is all-or-none when analyzed at the single channel level. In contrast, the effect of the antibody increases slowly to a maximum at a voltage-dependent rate when analyzed in whole cell voltage clamp (Vassilev et al, 1988). The progressive action of the antibody observed in whole cell experiments must represent the time-dependent diffusion and binding of the antibody to sodium channels rather than a time-dependent, progressive modification of channel properties.

Effects of Ab_{SP19} on single sodium channel currents at different test potentials. In our previous whole cell voltage clamp study, it was found that the antibody-induced slowing of inactivation was more prominent during depolarizations to more positive test potentials (> -30 mV). In this study, we found pronounced voltage-dependent effects on single channels which correlated well with those observed in the whole-cell experiments. Figure 6 shows single channel traces and ensemble average currents recorded at seven different test potentials under control conditions (Fig. 6A) and in the presence of Ab_{SP19} (Fig. 6B). Under control conditions, channel openings cluster at the onset of depolarization at all membrane potentials, although apparent channel re-openings are typically observed at test potentials of -50 mV and -60 mV. In the presence of Ab_{SP19}, both the frequency of channel opening and the probability of one or more channels being in the open state late in the depolarizing test pulses are significantly increased at all test potentials (Fig. 6B). However, the effect is much more striking at more positive test potentials. For example, in test pulses to -60 mV, channel openings are observed late in

the depolarizations in the absence of antibody, but their frequency and duration are increased in the presence of antibody. In contrast, in test pulses to -10 mV, single sodium channels activate and inactivate completely within 2 msec under control conditions, but continue to open throughout the 25 msec depolarizations in the presence of the antibody. As a result, the fraction of the ensemble average currents remaining at the end of the depolarization in the presence of Ab_{SP19} is progressively greater at more positive test potentials.

Inspection of the single channel current recordings made in the presence and absence of Ab_{SP19} (Fig. 6), suggests that Ab_{SP19} causes individual channel opening events to be prolonged. This effect is most striking at pulse potentials more positive than -30 mV where openings longer than 10 msec in duration are frequently observed in the presence of Ab_{SP19} but never in control. To make a quantitative assessment of the effect of Ab_{SP19} on the mean open times of the sodium channels, we analyzed the open time durations during test pulses to -20 mV, approximately the peak of the I-V curve. Figure 7 (panels A and B) shows frequency histograms of apparent mean open times obtained from single channel opening events recorded under control conditions (335 events, Fig. 7A) and in the presence of Ab_{SP19} (333 events, Fig. 7B). The data was fit well by a single exponential decay with a half-time of 0.69 msec in control and by a sum of two exponentials with half-times of 0.73 msec (46% of openings) and 5.62 msec (54% of openings) in the presence of Ab_{SP19}. We assume that the single channel openings having an unchanged mean open time in the presence of Ab_{SP19} are due to unmodified sodium channels, while those with prolonged open times are antibody-modified. Thus, these results indicate that binding of Ab_{SP19} induces approximately an eight-fold increase in the mean open time at -20 mV. The effect of Ab_{SP19} on mean open time is even greater at more positive membrane potentials since mean open times are prolonged even more markedly at more positive potentials in the presence of antibody, but change relatively little at more positive membrane potentials in control (Fig. 6, Aldrich et al, 1983; Horn & Vandenberg, 1984).

Steady-state inactivation and current voltage relationships in the presence of Ab_{SP19}. In order to determine whether Ab_{SP19} also prevented steady-state inactivation of Na channels, we carried out double-pulse experiments and recorded ensemble average currents. With no prepulse, the ensemble current rises rapidly to a peak and then declines to a plateau that is sustained throughout a 25 msec pulse to -20 mV (Fig. 7C, curve c) or -10 mV (Fig. 7D, curve c). In contrast, following a 250 msec prepulse to -60 mV (Fig. 7C) or a 100 msec prepulse to -30 mV (Fig. 7D), the early peak in the ensemble current is inactivated but, the sustained current is unaffected by the prepulse. Similar results are observed whether or not channel openings occur during the prepulse. Evidently, antibody-modified channels not only re-open repetitively during test pulses but also do not inactivate during 100 msec or 250 msec prepulses to less depolarized potentials. Because the peak in ensemble average currents at the beginning of test pulses in the presence of Ab_{SP19} has a similar time course to control Na currents and inactivates during depolarizing prepulses, we tentatively assign this current component to unmodified sodium channels.

The amplitudes of the ensemble-average currents were measured at the peak of sodium current and 10 msec after the beginning of the test pulse and plotted as a function of the applied test potential (Fig. 7E). No change in the voltage dependence of activation of single sodium channels by Ab_{SP19} was observed when peak currents were measured. The potential at which maximum sustained sodium currents were recorded appeared to be 5 to 10 mV more positive than that required for maximum peak currents in some recordings (Fig. 7E), but this was not a statistically significant difference in the recordings analyzed.

To determine the effect of Ab_{SP19} on slow inactivation of single sodium channels, the holding potential was varied and the amplitudes of ensemble average currents during 25 msec test pulses to -10 mV were measured at the peak of Na current and 10 msec after the beginning of the test pulse (Fig. 4F). The voltage dependence of slow inactivation of both the early and sustained sodium current components was unaffected by Ab_{SP19}. Thus, Ab_{SP19} completely inhibits fast sodium channel inactivation measured during a test pulse or during 100 or 250 msec prepulses, but does not markedly alter the voltage dependence of slow sodium channel inactivation processes.

The voltage dependence of the binding of Ab_{SP19} may follow directly from its inhibition of transition to the fast inactivated state. Our results show that Ab_{SP19} binds rapidly to its recognition site on the sodium channel in its resting conformation and prevents fast inactivation, but does not bind to this site when the sodium channel is inactivated. We conclude that the intracellular peptide segment between domains III and IV, which binds Ab_{SP19}, undergoes a conformational change during the process of inactivation making it inaccessible to Ab_{SP19}. The antibody inhibits inactivation by binding with high affinity to its recognition site in the "not inactivated" conformation and preventing or greatly slowing the transition to the fast inactivated state. The peptide segment recognized by Ab_{SP19} is required for rapid inactivation and is directly involved in that process. We propose that it may act as an "inactivation gate" by folding into the transmembrane pore of the sodium channel and occluding it in the inactivated state of the channel. This conformational transition is detected in our experiments as a loss of accessibility to Ab_{SP19}.

Inactivation of sodium channels is also inhibited by intracellular perfusion with proteases and amino-acid-specific reagents (reviewed in Armstrong, 1981). The action of proteases is slowed by depolarization suggesting that their site of action is also made inaccessible by inactivation of the sodium channel (Salgado et al 1985). Since the peptide segment recognized by Ab_{SP19} contains multiple pairs of basic amino acid residues which are favorable targets for proteolytic cleavage, proteases may inhibit inactivation by cleaving the α subunit at the site of action of Ab_{SP19}.

III. A Major Immunogenic Region of the Sodium Channel Near the Scorpion Toxin Receptor Site

Numerous neurotoxins interact specifically with multiple receptor sites on the sodium channel and have been instrumental in its purification and analysis of its electrophysiological properties (Catterall, 1986). Alpha scorpion toxins bind to neurotoxin receptor site 3 on sodium channels in a voltage-dependent manner and slow channel inactivation (Catterall, 1977; Catterall, 1979), suggesting that the toxin-sensitive region of the channel is involved in voltage-dependent conformational changes. A site of covalent attachment of photoreactive derivatives of the α-scorpion toxin from *Leiurus quinquestriatus* in the extracellular loop between transmembrane segments S5 and S6 in domain 1 of the sodium channel α subunit has been identified using anti-peptide antibodies directed against specific amino acid sequences (Tejedor & Catterall, 1989). Here we report that 5 monoclonal antibodies prepared against purified sodium channels specifically recognize a major immunogenic region in the same extracellular segment of the sodium channel α subunit that is involved in LqTx binding. As expected from the location of their antigenic site, these antibodies are able to block binding of ^{125}I-LqTx to its receptor site (see Section IV below). Definition of this extracellular antigenic region also distinguishes among models for the transmembrane folding of the α subunit and favors models with no more than six complete transmembrane segments per domain.

Peptides. Synthetic peptides (SP) and anti-peptide antibodies were prepared as previously described (Gordon et al, 1987; Gordon et al, 1988). Peptides used in this study were based on the following sequences from the deduced amino acid sequence of rat brain type II sodium channel α subunit (Kayano et al, 1988) : SP_{30-47}, AAEKAKRPKQERKDEDDE; SP_{76-84}, EPLEDLDPY; $SP_{317-334}$, DEYIEDKSHFYFLEGQND; $SP_{355-371}$, KAGRNPNYGYTSFDTFS; $SP_{382-401}$, TQDFWENLYQLTLRAAGKT; $SP_{427-445}$, AYEEQNQATLEEAEQKEA; $SP_{467-486}$, ASAESRDFSGAGGIGVFSE; $SP_{513-527}$, QAGEEEKEDAVRKSA; $SP_{676-692}$, TTETEIRKRRSSSYHVS; $SP_{1106-1126}$, PIALGESDFENLNTEEFSSE; $SP_{1429-1449}$, YAAVDSRNVELQPKYEDNLY; $SP_{1491-1508}$, TEEQKKYYNAMKKLGSKK; $SP_{1686-1703}$, KREVGIDDMFNFETFGNS; $SP_{1729-1748}$, PDCDPEKDHPGSSVKGDCGN; $SP_{1936-1954}$, KGKDEGTPIKEDIITDKL; $SP_{1987-2005}$, EKDKSEKEDKGKDIRESKK.

Monoclonal antibodies. Monoclonal antibodies were generated essentially following the procedure of Goding et al. (Goding, 1983). Balb/C mice were immunized subcutaneously with purified rat brain sodium channels (Hartshorne & Catterall, 1984) in soluble form or reconstituted into phosphatidylcholine vesicles (Talvenheimo et al, 1982). The initial injection contained antigen emulsified with Freund's complete adjuvant and was followed at two week intervals by boosts of antigen in Freund's incomplete adjuvant. Serum antibody levels were assayed by immunoprecipitation of ^{32}P-labeled sodium channels as outlined below. Boosts of antigen in buffer alone were given 5-7 days prior to fusion. Spleen cells from immunoreactive mice were collected and fused with SP20 mouse myeloma cells. After 7-10 days of selection in HAT medium, positive colonies were identified by radioimmune assay and cloned by limiting dilution. Ascites fluids were produced by injection of 10^7 cells into Balb/C mice primed 2 weeks earlier with 0.5 ml pristane. Antibodies 1A9 and 2E8 were raised against soluble sodium channels, whereas antibodies 1G11, 3B2 and 3G4 were raised against reconstituted sodium channels. All antibodies except 3B2 and 3G4 were produced in separate fusions. Antibodies were used in the form of ascites fluids or were purified from the ascites fluids by protein A-Sepharose chromatography as described by the manufacturer (Pharmacia). Based on their ability to bind protein A, all five monoclonal antibodies studied here are IgG (Goding, 1978).

Immunoblots. Purified sodium channels were subjected to SDS-PAGE in a resolving gel of 6% acrylamide under reducing conditions (Maizel, 1987) and electrophoretically transferred to Immobilon PVDF paper for 2 hrs at 70 V in 10 mM CAPS, 10% MeOH, pH 10.75 (Matsudaira, 1987). The immunoblots were incubated with antibody at a dilution of 1/100, followed by ^{125}I-labeled protein A, and bound protein A was visualized by autoradiography using Kodak XAR film as described (Rossie & Catterall, 1989).

Radioimmune assay. Radioimmune assays were performed as described previously (Costa & Catterall, 1989). Sodium channels were radiolabeled by phosphorylation with $\gamma^{32}P$-ATP using the catalytic subunit of cAMP-dependent protein kinase. Antibodies were incubated with synthetic peptides or unlabeled sodium channels in 75 mM NaCl, 2.5 mM EDTA, 25 mM Tris, 20 mM KF, 50 mM $NaPO_4$, 0.1% Triton X-100, pH 7.4 on ice for 3 h. A trace amount of ^{32}P-labeled sodium channel was added and the incubation continued overnight. Antibody-bound sodium channels were precipitated with protein A-Sepharose and ^{32}P was quantified by liquid scintillation counting.

Dot blots. Detergent-solubilized, purified sodium channels, untreated or denatured by boiling for 2 min with 3% SDS and 0.85 M β-mercaptoethanol, were applied directly to nitrocellulose and washed. The dot blots were probed with antibody (1/100 dilution) and ^{125}I-protein A as for immunoblots of SDS gels. Bound ^{125}I-protein A was visualized by autoradiography.

Recognition of the sodium channel α subunit by monoclonal antibodies. Five monoclonal antibodies generated in four separate fusions against purified rat brain sodium channels in soluble or reconstituted form were isolated on the basis of their ability to immunoprecipitate detergent-solubilized ^{32}P-labeled sodium channels. Although reconstituted channels were used as antigen in some cases, none of these antibodies bound reconstituted sodium channels preferentially (data not shown). Immunoblot analysis indicated that all of the monoclonal antibodies specifically recognized the α subunit of purified, SDS-denatured sodium channels (Fig. 8). All antibodies bound non-denatured sodium channels with greater affinity than denatured channels. Figure 9 compares recognition of non-denatured and SDS-denatured sodium channels by antibody 2E8 in a solid phase ELISA assay. At each concentration of sodium channel tested, non-denatured channels bound more antibody. Similar results were obtained with all five monoclonal antibodies. Pretreatment of the nitrocellulose with 3% SDS prior to sample application did not influence binding, indicating that the differences measured are not simply due to nonspecific influence of SDS pretreatment on antibody binding. Thus, as is common for monoclonal antibodies, these anti-sodium channel antibodies bind preferentially to the native conformation of the detergent-solubilized α subunit.

Immunoprecipitation of sodium channels by monoclonal antibodies is blocked by SP317-334 and SP382-401. In order to determine the region of the α subunit recognized by the monoclonal antibodies, we tested the ability of 50 μM concentrations of synthetic peptides representing approximately 20-residue segments of the amino acid sequence of the α subunit to block immunoprecipitation of detergent-solubilized, ^{32}P-labeled sodium channels. Of 15 peptides representing sequences from the amino to the carboxy terminus, only SP317-334 and SP382-401, derived from the first homologous domain of the channel α subunit, inhibited immunoprecipitation by all five antibodies significantly (Fig.10). All other peptides tested, including SP355-371, had inconsistent or no effects on immunoprecipitation of sodium channels. The observation that SP317-334 and SP382-401, but not SP355-371, can prevent interaction of the monoclonal antibodies with sodium channels implies that these antibodies recognize a conformational epitope which includes peptide segments contained within residues 317-334 and 382-401, but not residues 355-371.

Binding of each monoclonal antibody to SP317-334 and SP382-401 was compared to that of detergent-solubilized purified sodium channels in Fig. 11. In radioimmune assays, unlabeled sodium channels blocked immunoprecipitation of ^{32}P-labeled channels by monoclonal antibodies in a concentration-dependent manner, with 50% inhibition at 2 to 10 nM and complete inhibition at 20 nM to 0.1 μM. Much higher concentrations of synthetic peptides were required to block interaction of the antibodies with sodium channels. Concentrations of 0.1 to 50 μM of the peptides progressively inhibited immunoprecipitation of ^{32}P-labeled sodium channels. Immunoprecipitation by antibodies 1G11, 2E8, and 3B2 was blocked more than 90% by 50 μM SP317-334. In all other cases, inhibition by the peptides was incomplete at 50 μM, the highest concentration tested. For all antibodies, SP317-334 was equal to or greater in potency than SP382-401 in blocking sodium channel binding.

Effect of deglycosylation on antibody binding. Asparagine residues at positions 284, 290, 296, 302, 307, and 339 in RII sodium channels are potential sites of N-linked glycosylation (Noda et al, 1986a). Previous results (Tejedor & Catterall, 1989) indicate that this region of the sodium channel is heavily glycosylated because removal of sialic acid with neuraminidase reduces its apparent mass by 24 kDa. We examined whether this large mass of sialic acid residues contributes to the antigenic determinants for monoclonal antibody binding or hinders access of the antibodies to their binding sites. Treatment with neuraminidase to remove sialic acid residues enhanced immunoprecipitation

of sodium channels by antibodies raised against $SP_{317-334}$, a peptide segment immediately adjacent to the sites of glycosylation on the α subunit, but had no effect on immunoprecipitation by antibodies against $SP_{427-445}$ (Fig. 12). In contrast, neuraminidase treatment did not influence binding of any of the monoclonal antibodies (Fig. 12), despite the fact that the monoclonal antibodies also recognize at least part of residues 317-334 in the α subunit. These results suggest that sialic acid does not contribute to recognition of this region by these monoclonal antibodies and does not hinder access to their binding sites appreciably.

A major immunogenic region in domain I of the sodium channel α subunit. Our results show that all five independent monoclonal antibodies raised against purified rat brain sodium channels in three separate fusions specifically bind to a region of the first homologous domain of the α subunit. Binding of these antibodies to the sodium channel is inhibited by 1 to 50 μM $SP_{317-334}$ and $SP_{382-400}$, but not by $SP_{355-371}$. Thus, the site of recognition for these antibodies is a conformational epitope composed of discontinuous determinants that include polypeptide segments within residues 317-334 and 382-400. The intervening residues 355-371 apparently do not participate in the binding site for these antibodies. The antibodies bind $SP_{317-334}$ and $SP_{382-400}$ with 100- to 1000-fold lower affinity than the sodium channel itself. Relatively low affinity of synthetic peptides for monoclonal antibodies that recognize conformationally dependent epitopes has been observed by a number of investigators (Benjamin et al, 1984). Evidently the antigenic site(s) for these antibodies contain additional amino acid residues or the synthetic peptides do not fold in the same conformation as the α subunit.

The striking observation that all five monoclonal antibodies recognize the same region of the sodium channel is reminiscent of the main immunogenic region of the nicotinic acetylcholine receptor, a region of the α subunit toward which an extraordinarily large portion of naturally occurring and experimentally generated antibodies are directed (Tzartos & Lindstrom, 1980; Gordon RD et al, 1987). This phenomenon has not previously been observed in the case of voltage-sensitive sodium channels. Analysis of a larger pool of anti-sodium channel antibodies will be required to determine whether the extracellular segment of the first homologous domain of the α subunit between proposed transmembrane segments S5 and S6 can be designated the main immunogenic region of the sodium channel in analogy with previous work on the acetylcholine receptor. In any case, the apparent immunodominance of this region of the rat brain sodium channel impedes production of mouse monoclonal antibodies that recognize a broad spectrum of channel domains.

IV. Antibody Mapping of the α-Scorpion Toxin Receptor Site. Block of Toxin Binding by Antibodies

In previous studies, the site of covalent attachment of photoreactive derivatives to the α subunit has been localized by immunoprecipitation with site-directed anti-peptide antibodies to the extracellular loop between proposed transmembrane segments S5 and S6 of domain I (Tejedor & Catterall, 1989) In the present experiments, we have analyzed the effects of a series of site-directed anti-peptide and monoclonal antibodies on the voltage-dependent binding of LqTx to sodium channels to define regions of the channel structure that are located on its extracellular surface and are required for toxin binding at higher resolution.

^{125}I-LqTx Binding to Reconstituted Sodium Channel. Rat brain sodium channels purified through the step of chromatography on wheat germ agglutinin-Sepharose (Hartshorne & Catterall, 1984) at concentrations of 300-400 pmol/ml in a solution containing 25 mM Hepes-Tris (pH 7.4), 100 mM Na_2SO_4, 0.4 mM $MgSO_4$, 157 mM N-

acetylglucosamine, 4 μM tetrodotoxin, 1.65% Triton X-100, 0.19% phosphatidylcholine, and 0.12% phosphatidylethanolamine were reconstituted in phospholipid vesicles as previously described (Tamkun et al, 1984; Feller et al, 1985). After preincubation of reconstituted vesicles with preimmune IgG, site-directed antibody, or monoclonal antibody, ^{125}I-LqTx binding assays were performed essentially as described previously (Tamkun et al, 1984). Briefly, assays were initiated by the addition of 40 μL of preincubation mixture to 160 μL of a solution containing 0.23 nM ^{125}I-LqTx, 105 mM Tris-SO_4, 0.5 mM $MgSO_4$, 25 mM Hepes-Tris, 150 mM sucrose, and 4 mg/ml BSA, pH 7.4. The sucrose concentration was adjusted to maintain osmolarity equal to the intravesicular medium. The reaction mixture was then incubated for five minutes at 37°C, diluted with 3 ml of wash buffer containing 163 mM choline chloride, 0.8 mM $MgSO_4$, 1.8 mM $CaCl_2$, 5 mM Hepes (adjusted to pH 7.4 with Tris base), 1 mg/ml BSA, and sucrose sufficient to maintain osmolarity, filtered over GF/F filters under vacuum pressure, and washed three more times with the same wash buffer. Nonspecific toxin binding was determined in the presence of 1 μM unlabeled LqTx and accounted for 20-40% of the total binding. Approximately 75% of the nonspecific binding is to GF/F filters alone.

^{125}I-LqTx Binding to Rat Brain Synaptosomes. Rat brain synaptosomes were prepared as previously described (Kanner, 1978) and stored at -80°C until used. After preincubation of synaptosomes with IgG as described in each figure legend, ^{125}I-LqTx binding was quantitated as described for reconstituted sodium channel. Incubations containing monoclonal antibodies were performed at 37°C for 30 minutes instead of 5 minutes. Nonspecific binding was determined in the presence of 1 μM LqTx and accounted for 10-25% of the total binding.

Inhibition of binding of ^{125}I-LqTx by site-directed antibodies. Six site-directed antibodies (IgG) that recognize different proposed extracellular regions of the R_{II} sodium channel α-subunit were evaluated for their ability to inhibit ^{125}I-LqTx binding to sodium channels in reconstituted phospholipid vesicles and synaptosomes (Fig. 13). Preincubation of purified sodium channels reconstituted in phospholipid vesicles with three of the six antibodies, $Ab_{355-371}$, $Ab_{382-400}$, and $Ab_{1686-1703}$, inhibited ^{125}I-LqTx binding by 28%, 55%, and 54%, respectively (Fig. 13A). Similar levels of antibody-mediated inhibition of ^{125}I-LqTx binding were observed when partially purified sodium channel was preincubated for four hours at 4°C with the same quantity of these antibodies prior to reconstitution and toxin binding assays (data not shown). $Ab_{317-334}$, $Ab_{1429-1449}$, and $Ab_{1729-1748}$ did not have significant effects on LqTx binding (Fig. 13A). Ab_{SP19}, an antibody recognizing the proposed intracellular segment of the α-subunit between homologous domains III and IV (residues 1541-1558) associated with sodium channel inactivation (Vassilev et al, 1988), also had no effect on toxin binding (data not shown). Similar results were observed using rat brain synaptosomes (Fig. 13B). In this case, $Ab_{355-371}$, $Ab_{382-400}$, and $Ab_{1686-1703}$ inhibited ^{125}I-LqTx binding by 33%, 29%, and 27%, respectively, while the other three antibodies had no effect. $Ab_{355-371}$ and $Ab_{382-400}$ are directed against synthetic peptides corresponding to amino acid residues which are located on the proposed extracellular loop between transmembrane segments S5 and S6 of homologous domain I near the site previously identified by covalent attachment of LqTx derivatives (Tejedor & Catterall, 1989). $Ab_{1686-1703}$ is directed against a synthetic peptide corresponding to amino acid residues located on the proposed extracellular segment between transmembrane segments S5 and S6 in homologous domain IV. Since these three antibodies inhibit LqTx binding while other closely related anti-peptide antibodies do not, our results suggest that the corresponding extracellular segments of domains I and IV interact in forming the receptor site for LqTx.

Concentration-effect curves for inhibition of LqTx binding to either reconstituted rat brain sodium channel or synaptosomes by $Ab_{355-371}$ indicate that inhibition is concentration-dependent (Fig. 14). Using reconstituted vesicles, EC_{50} values of 0.51+/-

0.21 μM, 0.39+/-0.12 μM, and 0.57+/-0.20 μM and maximal inhibition of 39%, 36%, and 47% were obtained for $Ab_{355-371}$, $Ab_{382-400}$, and $Ab_{1676-1703}$, respectively (Fig. 14A). Higher EC_{50} values of 0.65+/-0.15 μM, 2.0+/-0.66 μM, and 1.35+/-0.38 μM and similar maximal levels of inhibition of 29%, 43%, and 33% were observed using rat brain synaptosome preparations (Fig. 14B). It should be noted that the concentrations of antibody listed correspond to total IgG isolated from antisera and therefore estimated EC_{50} values substantially exceed the true values for the active antibodies. Definition of maximal levels of inhibition was difficult because of limitations in the amount of antibody that could be added during the preincubation period. However, in all cases the curves appear to approach saturation of the antibody effect.

The extent of inhibition of LqTx binding by site-directed antibodies was not increased by treatments designed to improve their access to their binding sites. Neuraminidase treatment of purified sodium channel to remove sialic acid residues prior to reconstitution did not result in enhanced inhibition of toxin binding, and smaller Fab fragments generated by papain treatment of IgG produced similar levels of inhibition of ^{125}I-LqTx binding to reconstituted vesicles as native IgG. Moreover, the effects of maximal concentrations of $Ab_{355-371}$, $Ab_{382-400}$, and $Ab_{1676-1703}$ were not additive. These results suggest that the anti-peptide antibodies completely inhibit LqTx binding to sodium channels to which they can gain access and bind, but that a fraction of sodium channels do not bind the anti-peptide antibodies.

Inhibition of ^{125}I-LqTx binding by monoclonal antibodies. Our laboratory has recently characterized five independent mAb which recognize epitope(s) in the extracellular loop of homologous domain I situated between transmembrane segments S5 and S6. The binding of these antibodies to sodium channels is prevented by peptides $SP_{317-334}$ and $SP_{382-400}$ but not by 11 other sodium channel peptides tested (Rossie et. al., submitted for publication). All five mAb inhibit ^{125}I-LqTx binding to sodium channels in synaptosomes in a concentration-dependent manner (Fig. 15). Maximal levels of inhibition of 94%, 98%, 86%, 97%, and 89% were observed for monoclonal antibodies 1G11, 1A9, 2E8, 3B2, and 3G4, respectively. EC_{50} values of 1.26+/-0.10 μM, 0.56+/-0.13 μM, 0.57+/-0.06 μM, 0.77+/-0.19 μM, and 0.39+/-0.06 μM were obtained for these antibodies, respectively. Collectively, these results indicate that mAb recognizing the same extracellular loop as $Ab_{355-371}$ and $Ab_{382-400}$ inhibit ^{125}I-LqTx binding to sodium channels in synaptosomes nearly completely at micromolar concentrations. These results provide additional support for the conclusion that this extracellular segment is required for formation of neurotoxin receptor site 3.

Time course of inhibition of ^{125}I-LqTx binding. To examine the time course of antibody inhibition, toxin binding to either reconstituted vesicles or synaptosomes was measured after the indicated periods of preincubations with 1 μM $Ab_{382-400}$, 0.4 μM mAb3G4 (not shown), or 6 μM mAb3G4 (Fig. 16A). The time courses for inhibition by $Ab_{382-400}$ are best described as monoexponential for both reconstituted vesicles and synaptosomes. Maximal levels of inhibition are obtained by 120-180 minutes of preincubation and half-times of 78 and 38 minutes were observed using vesicles and synaptosomes, respectively. The time course for inhibition by 6 μM 3G4 is best described as biexponential with similar amplitudes of the fast (60%, $t_{1/2}$ = 1.2 and 0.2 min) and slow (30%, $t_{1/2}$ = 23 and 35 min) components in reconstituted vesicles and synaptosomes, respectively.

Influence of mAb on the concentration dependence of ^{125}I-LqTx binding. The effect of the mAbs on LqTx binding is not reversible within the time of our experiments (data not shown). If the mAbs act as slowly reversible competitive ligands at the scorpion toxin receptor site, their effect on ^{125}I-LqTx binding should be observed as a reduction in the number of toxin binding sites and they should have no effect on the rate of

dissociation of previously bound toxin. Fig. 16B shows saturation isotherms for ^{125}I-LqTx binding to rat brain synaptosomes in the absence and presence of 0.5 μM mAb 1A9. Similar K_d values of 1.5 +/- 0.3 and 2.1 +/- 0.3 nM were observed in the absence and presence of mAb, respectively, but a 75% reduction in the number of binding sites was observed in the presence of mAb. Addition of 1 μM 1A9 had no effect on the rate of dissociation of previously bound ^{125}I-LqTx (data not shown) These results are consistent with an action of the mAbs as slowly reversible competitors for LqTx binding sites. All five monoclonal antibodies blocked binding of ^{125}I-LqTx to purified and reconstituted sodium channels with up to 81% inhibition at 5 μM (Fig. 6). The antibody concentrations required for half-maximal inhibition ranged from 0.11 to 1.4 μM . These results provide independent evidence for location of both a major immunogenic region and a portion of the α-scorpion toxin receptor site between residues 317 and 400 in the extracellular loop between segments S5 and S6 of domain I of the sodium channel α subunit.

Interaction of extracellular segments of domains I and IV in forming the α-scorpion toxin receptor site. Photoreactive derivatives of LqTx were previously shown to be incorporated into the extracellular segment of the sodium channel between amino acid residues 317 and 400 in domain I (Tejedor & Catterall, 1989). We show here that antipeptide antibodies recognizing residues 355-371 and 382-400 are effective inhibitors of LqTx binding while antibodies recognizing the adjacent residues 317-335 and several other sodium channel segments are not. These results implicate the peptide segment from residues 355 to 400, immediately adjacent to proposed transmembrane segment S6, in α-scorpion toxin binding.

Five independent mAbs raised against purified rat brain sodium channels recognize epitope(s) formed by peptide segments between amino acid residues 317 to 400 (Rossie et al, submitted for publication). Binding of these mAbs to sodium channels is blocked by synthetic peptides $SP_{317-335}$ and $SP_{382-400}$, but not by $SP_{355-371}$. Evidently, epitope(s) recognized by these mAbs are formed by interaction of two discontinuous peptide segments containing residues 317-335 and 382-400. We show here that these mAbs are effective inhibitors of LqTx binding and that their mechanism of inhibition is consistent with slowly reversible interaction at the α-scorpion toxin receptor site. Since $Ab_{317-335}$ does not inhibit LqTx binding appreciably, the combination of the results with antipeptide antibodies and mAbs points to amino acid residues 371 to 400 as playing an essential role in α-scorpion toxin binding.

Binding of α-scorpion toxins to the sodium channel is conformationally dependent (Catterall, 1977; Tamkun et al, 1984; Feller et al, 1985), and it was predicted (Tejedor & Catterall, 1989) that multiple polypeptide segments from different regions of the primary structure might contribute to formation of neurotoxin receptor site 3. Our present results show that $Ab_{1686-1703}$ is an effective inhibitor of LqTx binding while several other anti-peptide antibodies including $Ab_{1729-1748}$ are not. Amino acid residues 1686-1703 are located in the extracellular segment between proposed transmembrane segments S5 and S6 of domain IV near the junction with S5. Thus, we propose that amino acid sequences from these two distant regions of the primary structure of the sodium channel α subunit (Fig. 18A) participate in formation of neurotoxin receptor site 3.

Although domains I and IV of the sodium channel α-subunit are distant from each other in the primary structure of the channel, the four homologous domains defined in the primary structure are proposed (Noda et al, 1986a; Greenblatt et al, 1985; Guy & Seetharamulu, 1986) to be organized in a square array around a central transmembrane pore placing domains I and IV adjacent to each other in the three dimensional structure of the channel protein (Fig. 18B). Our results provide the first experimental support for this widely accepted proposal. Scorpion toxins are small elliptical molecules of approximately 50x40x30 A (Fontecilla-Camps et al, 1988). Their binding surface is thought to extend

over part of one face of the molecule. The inhibition of LqTx binding by anti-peptide and monoclonal antibodies described here indicates that this small binding face may interact with a receptor site formed by the close apposition of residues 371-400 of domain I and residues 1686-1703 of domain IV of the sodium channel α subunit (Fig. 18B).

A major immunogenic region is located near the α-scorpion toxin receptor site. All five monoclonal antibodies that we have studied effectively block binding of ^{125}I-labeled LqTx to purified and reconstituted sodium channels. Since the receptor site for α-scorpion toxins has previously been shown to include segments of the amino acid sequence between residues 317 and 400 (Hartshorne & Catterall, 1984), inhibition of binding of LqTx by these monoclonal antibodies provides independent support for the location of their antigenic site in this region of the sodium channel α subunit. Relatively high concentrations of monoclonal antibodies are required to inhibit LqTx binding to reconstituted sodium channels compared to the concentrations required for immunoprecipitation of detergent-solubilized sodium channels. Alpha scorpion toxins bind with high affinity to reconstituted sodium channels, but not to detergent -solubilized sodium channels (Gordon RD et al, 1988; Rossie & Catterall, 1987). Thus, the conformation of this region of the α subunit differs substantially between detergent-solubilized and reconstituted sodium channels, and this conformational difference is reflected in the different affinity for the monoclonal antibodies. Alpha scorpion toxins slow the rate of inactivation of sodium channels during a maintained depolarization (reviewed in Catterall, 1979). Thus, it is anticipated that this region of the channel is involved in the conformational coupling of channel activation to inactivation (Catterall, 1977; Catterall, 1979). It will be of interest to examine the physiological effects of these monoclonal antibodies on sodium channel function. In addition, these monoclonal antibodies are now prime candidates for agents to block the actions of scorpion toxins and sea anemone toxins on the sodium channel.

Transmembrane organization of amino acid sequences between transmembrane segments S5 and S6. Proposals for the transmembrane organization of sodium channel α subunits (Noda et al, 1986a; Greenblatt et al, 1985; Guy & Seetharamulu, 1986; Fig. 19) all suggest that the N- and C-termini and inter-domain segments are cytoplasmic in orientation. Direct support for this orientation has come from localization of antibody binding sites (Gordon RD et al, 1988; Gordon RD et al, 1988), cAMP-dependent phosphorylation sites (Rossie et al, 1987), and sites of channel inactivation (Vassilev et al, 1988). These models all propose that hydrophobic segments S1 through S6 are transmembrane segments, although there is no direct experimental evidence to support these proposals. In addition, two models (Greenblatt et al, 1985; Guy & Seetharamulu, 1986) propose that amino acid sequences between transmembrane segments S5 and S6 form two additional complete or partial transmembrane segments (Fig. 19). Because scorpion toxins clearly bind to the extracellular surface of the sodium channel, localization of their receptor sites will contribute to definition of its transmembrane orientation. Our previous work showed that at least part of the amino acid sequence between transmembrane segments S5 and S6 of domain I was extracellular and could be covalently labeled by photoreactive LqTx derivatives (Tejedor & Catterall, 1989). Our present studies define this extracellular region more clearly.

High affinity binding of α-scorpion toxins requires incorporation of the channel into an appropriate phospholipid environment and establishment of an internal negative membrane potential (Feller et al, 1985). Therefore, we can assume that all sodium channels to which we measure binding of LqTx are appropriately incorporated into sealed reconstituted phospholipid vesicles or synaptosomes with their extracellular surface facing outwards. Under these conditions, we find that anti-peptide and monoclonal antibodies recognizing amino acid residues 371-400 can bind to sodium channels and inhibit LqTx binding. These results provide strong evidence that these amino acid sequences in domain

I are available to antibodies on the extracellular surface of the channel protein and are not buried deep within the protein or the phospholipid bilayer. Thus, our results do not support the proposals (Greenblatt et al, 1985; Guy & Seetharamulu, 1986) that these amino acid residues form partial or complete transmembrane segments in domain I. On the basis of these data, we favor the hypothesis that there are six transmembrane segments in domain I (Noda et al, 1986a; Meves et al, 1986), and probably in each homologous domain. Thus, the amino acid sequences between transmembrane segments S5 and S6 in each domain would be fully extracellular (Fig. 19B) and available to participate in formation of receptor sites for the many other neurotoxins that act on the extracellular surface of the sodium channel.

Scorpion toxin action and the site of coupling of activation to inactivation. Alpha scorpion toxins slow sodium channel inactivation specifically (Meves et al, 1986; Strichartz et al, 1987), but the voltage-dependence of their binding closely follows that of channel activation (Catterall, 1979). Based on these results, we have previously proposed that these toxins bind to a receptor site whose conformation changes upon channel activation and slow inactivation by preventing normal coupling of activation to subsequent inactivation (Catterall, 1977; Catterall, 1979). Therefore, we expect that the site of α-scorpion toxin binding is located near regions of the channel that are critical for the coupling of activation to inactivation. Voltage-dependent activation of sodium channels is thought to involve sequential voltage-driven conformational changes initiated by the force of the electrical field acting on highly conserved gating charges located in the S4 transmembrane segments in each domain (Catterall, 1986; Guy & Seetharamulu, 1986). Neutralization of these charges in the S4 segment of domain I by site-directed mutagenesis causes a progressive reduction of activation gating charge (Stuhmer et al, 1989) indicating that this segment plays an important role in initiating channel activation. Fast inactivation of the sodium channel is thought to be mediated by an inactivation gate formed by the intracellular segment between domains III and IV (Vassilev et al, 1988; Stuhmer et al, 1989; Vassilev et al, 1989). The location of the α-scorpion toxin receptor site at a point of interaction between the extracellular segments of domains I and IV places the toxin in a position to interact with the S4 gating charges in these two domains and to slow or prevent the coupling of activation gating charge movements in domain I to conformational changes in domain IV that initiate closing of the inactivation gating segment. Further probing of the toxin receptor site may help to define the mechanism of activation-inactivation coupling.

Figure 1. *Functional expression of rat brain sodium channels in transfected CHO cells. A. RNase protection.* Autoradiogram of α_{IIA} transcripts protected from RNAse digestion in seven independent transfected CHO lines. Cytoplasmic RNA was isolated from detergent-solubilized CHO cells by NaOAc, pH 5, ETOH precipitation (Rassmussen et al, 1987). Fifteen μg CHO RNA, 10 μg tRNA or 2 μg brain polyA+ RNA was hybridized to an 817 nucleotide probe containing nucleotides 50-831 (Auld et al, 1988) of the α_{IIA} mRNA, and treated with RNase A and RNase T1 as described (Melton et al, 1984). Denatured RNA duplexes were electrophoresed on a 5% polyacrylamide gel. Lane 1, size markers (tick marks indicate 1018, 516/506, and 394 nucleotides, respectively); lane 2, probe; lane 3, tRNA; lane 4, brain polyA+ RNA; lanes 5-11, transfected CHO lines PVA1 PVA7. **B.** Messenger RNA blot. CHO cells were transfected with pVA222 or the pECE vector and stable cell lines were established as described (Ellis et al, 1986). RNA was isolated from cells by homogenization in guanidine thiocyanate and centrifugation through CsCl (Glisen et al, 1973). Ten μg of total RNA was electrophoresed in polyacrylamide gels containing 2.2 M formaldehyde, transferred to nitrocellulose, and hybridized to a cRNA probe containing an insert spanning nucleotides 3361-5868 of the R_{IIA} α subunit (Auld et al, 1988). Hybridization was performed in 6X SSC, 50% formamide, 50 mM Tris-HCl, 10X Denhardt's solution, 0.5% SDS at 68°C. After hybridization, the blot was washed at room temperature in 2X SSC, 0.5% SDS, and in 0.2X SSC, 0.5% SDS at 68°C. After washing, the nitrocellulose filters were exposed for autoradiography for 1 hr (lane 1) or 8 hr (lanes 2-4) at -80°C. Lane 1, total brain RNA; lane 2, CP1 RNA; lane 3, PVA4 RNA; lane 4, PVA1 RNA. **C.** Sodium currents in PVA1 (panel 1), PVA4 (panel 2), and CP1 (panel 3) cells. Inward sodium currents were recorded during step depolarizations to -38, -29, -19, -10, 0, 19, 38, 57, 77 and 86 mV for 16 ms from a holding potential of -67 mV. Pulses to +77 and +86 mV are omitted for PVA4 cell. Each voltage step was preceded by a 200 ms long prepulse to -100 mV. Calibration marks indicate 2 msec and 100 pA. **D.** Families of sodium currents in PVA1 cells evoked by voltage steps ranging from -40 to +50 mV in 10 mV steps as in panel C, before (panel 1), during (panel 2), and after (panel 3) exposure to 100 nM TTX. Calibration marks indicate 2 msec and 100 pA.

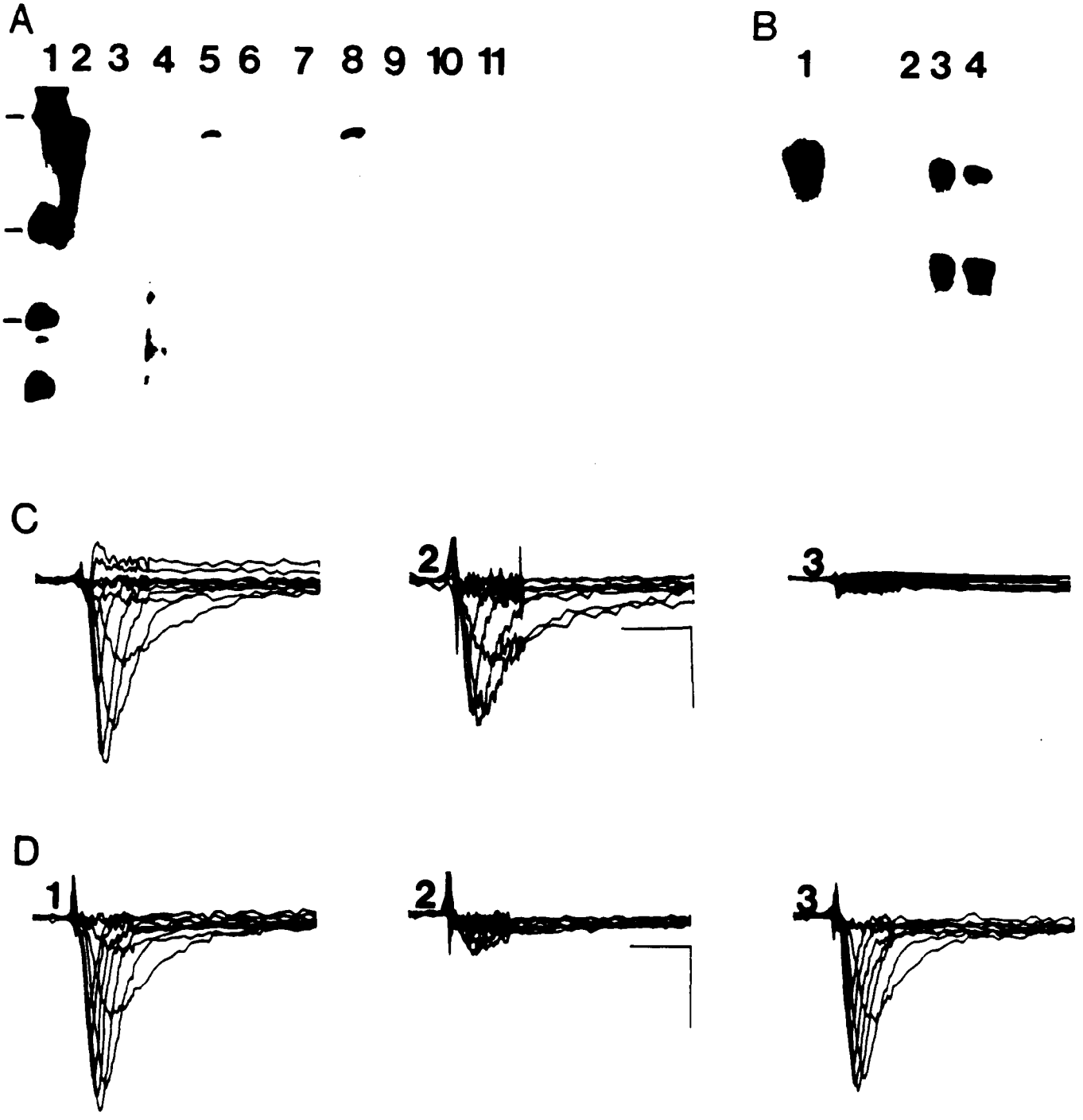
A
1 2 3 4 5 6 7 8 9 10 11
B
1
2 3 4
C
2
3
D
1
2
3

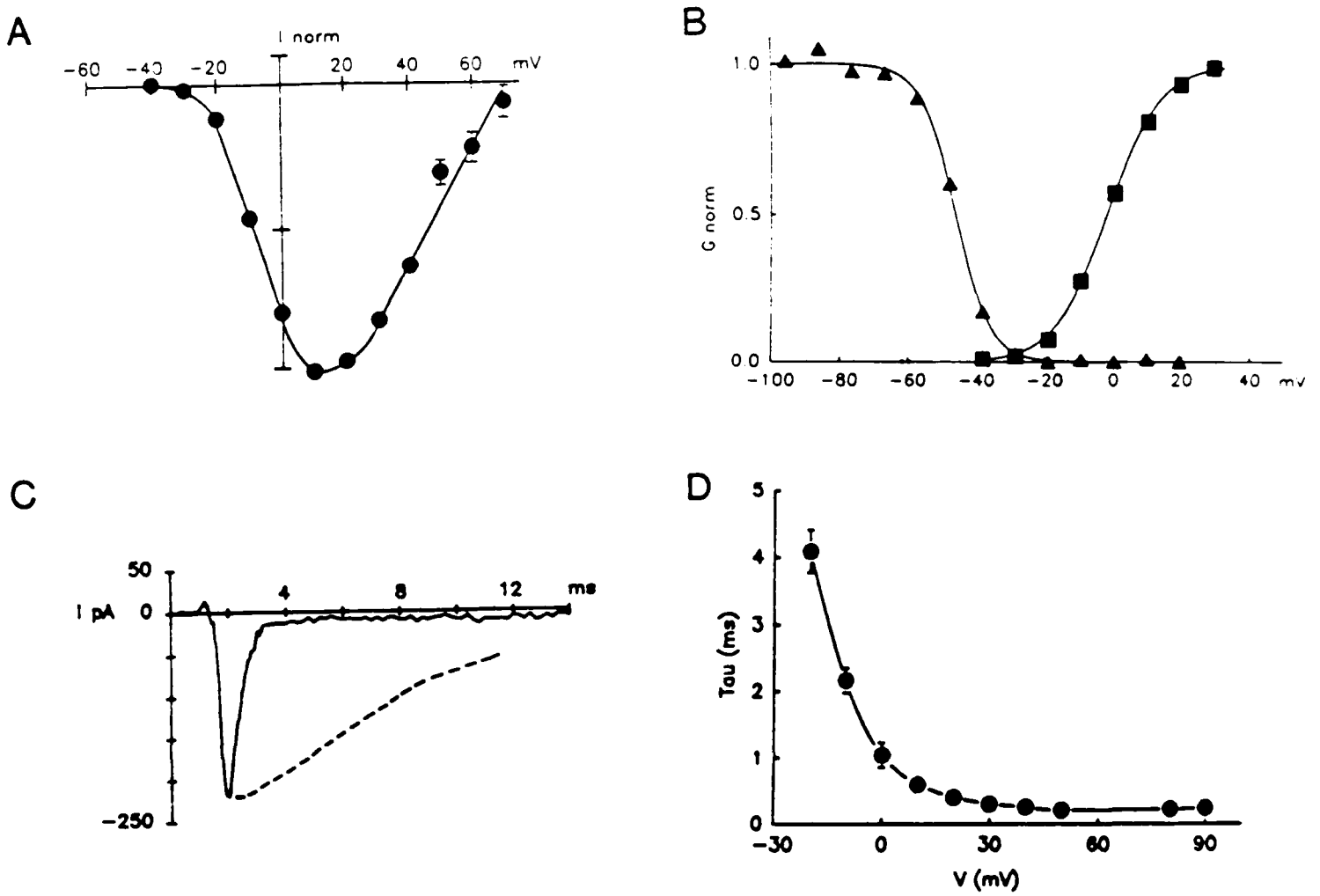

Figure 2. *Properties of sodium currents in transfected CHO cells.* **A.** Mean, normalized sodium current I-V relationship from PVA1 cells. Peak sodium currents measured from current families similar to those shown in Fig. 1C were normalized to peak current, averaged on a voltage-by-voltage basis, and plotted as a function of voltage during the test pulse. Error bars represent S.E.M. **B.** Normalized conductance-voltage (G-V) and inactivation curves from a PVA1 cell. G-V curves were from obtained sodium current families recorded at different test pulse potentials as in Fig. 1C. Conductances, G, (squares) were obtained from normalized peak current values, I, the test pulse voltage, V, and the measured IV curve reversal potential, V_{rev}, according to the equation: $G(V) = I / (V - V_{rev})$. Inactivation curve was determined using 200 ms long prepulses to the indicated membrane potentials followed by a test pulse to +10 mV. Normalized peak currents are plotted as a function of prepulse potential (triangles). Curves through the points are least-squares fits to normalized to: $1 / \{ 1 + \exp[(V - V_{5}) / k]\}$ where V_{5} is the voltage of half activation and k gives the steepness of voltage-dependence. Best fit values were- Activation: V_{5} = +2.0 mV, k = -7.55 mV; Inactivation: V_{5} = -45.96, k = 5.06. **C.** Comparison of the time courses of sodium currents mediated by RIIA α subunits expressed in PVA1 cells and in *Xenopus* oocytes. Solid trace, inward current evoked by a voltage pulse to +10 mV in a PVA1 cell. Broken trace, approximate time course of I_{Na} in a *Xenopus* oocyte at the same test potential, as previously reported (Auld et al, 1988). **D.** Time constants of macroscopic inactivation of I_{Na}. Points were obtained by least squares fits of single exponentials to the decline of I_{Na} during depolarizations. Points represent the means of 6 to 9 determinations except at +80 and +90 mV where n = 2. Error bars ($\pm$S.E.M.) are not shown when smaller than the symbol size.

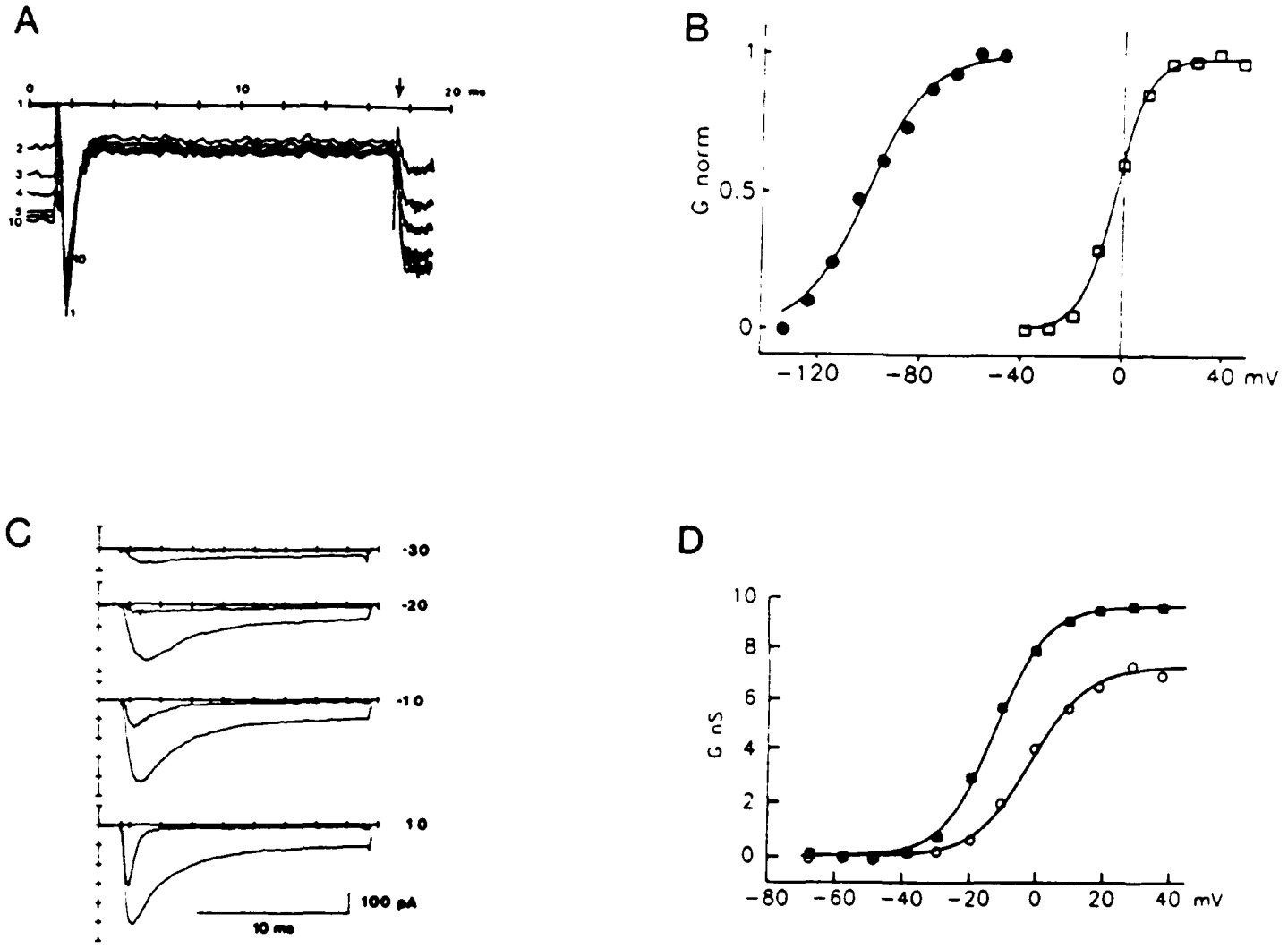

Figure 3. *Toxin effects on sodium channels expressed in CHO cells.* **A.** Currents recorded during 10 successive depolarizations from a holding potential of -100 mV to +20 mV applied at 5 Hz in the presence of 100 μM veratridine. Current traces shown were recorded during pulses 1-5, 7, and 10 as indicated adjacent to each trace. Each trace represents the pulse-wise average of 5 successive pulse trains separated by 30 s to 1 min quiescent intervals. Similar trains of control pulses (not shown) caused no pulse-wise changes in peak or holding current. **B.** Voltage-dependence of veratridine-modified sodium channels. Control conductance-voltage curve (open squares) was obtained as described in Fig. 2B. During exposure to 100 μM veratridine, approximate mean conductances (filled circles) were obtained by developing a population of veratridine modified channels using a train of 10 successive, 2 ms long pulses as in panel A. Membrane potential was then stepped to -160 mV for 17 ms followed by pulses to the test potentials shown. Veratridine-modified channels close slowly in comparison to the 17 ms spent at -160 mV and therefore remain open during the subsequent test pulses. Peak current values were measured and transformed into normalized conductances as in Fig. 2B. **C.** Effect of the α-scorpion toxin from *Leiurus quinquestriatus* on sodium currents. The time course of inward sodium current was measured at the indicated test potentials before and during exposure to purified (Catterall, 1976) LqTx. At each membrane potential, the larger sodium current was recorded in the presence of LqTx. After control recordings, 2 μl of 70 μM toxin was added near the cell. Toxin concentration for uniform distribution in the bath volume was 140 nM. **D.** G-V relationships before and during exposure to LqTx. Same experiment as in panel C. Conductance values (unnormalized) and fit curves were obtained as in Figure 2B. Best fit values were: control (open circles), $V_{.5}$ = -0.45 mV, k = -8.9 mV; LqTx (closed squares), $V_{.5}$ = -9.9 mV, k = -7.7 mV.

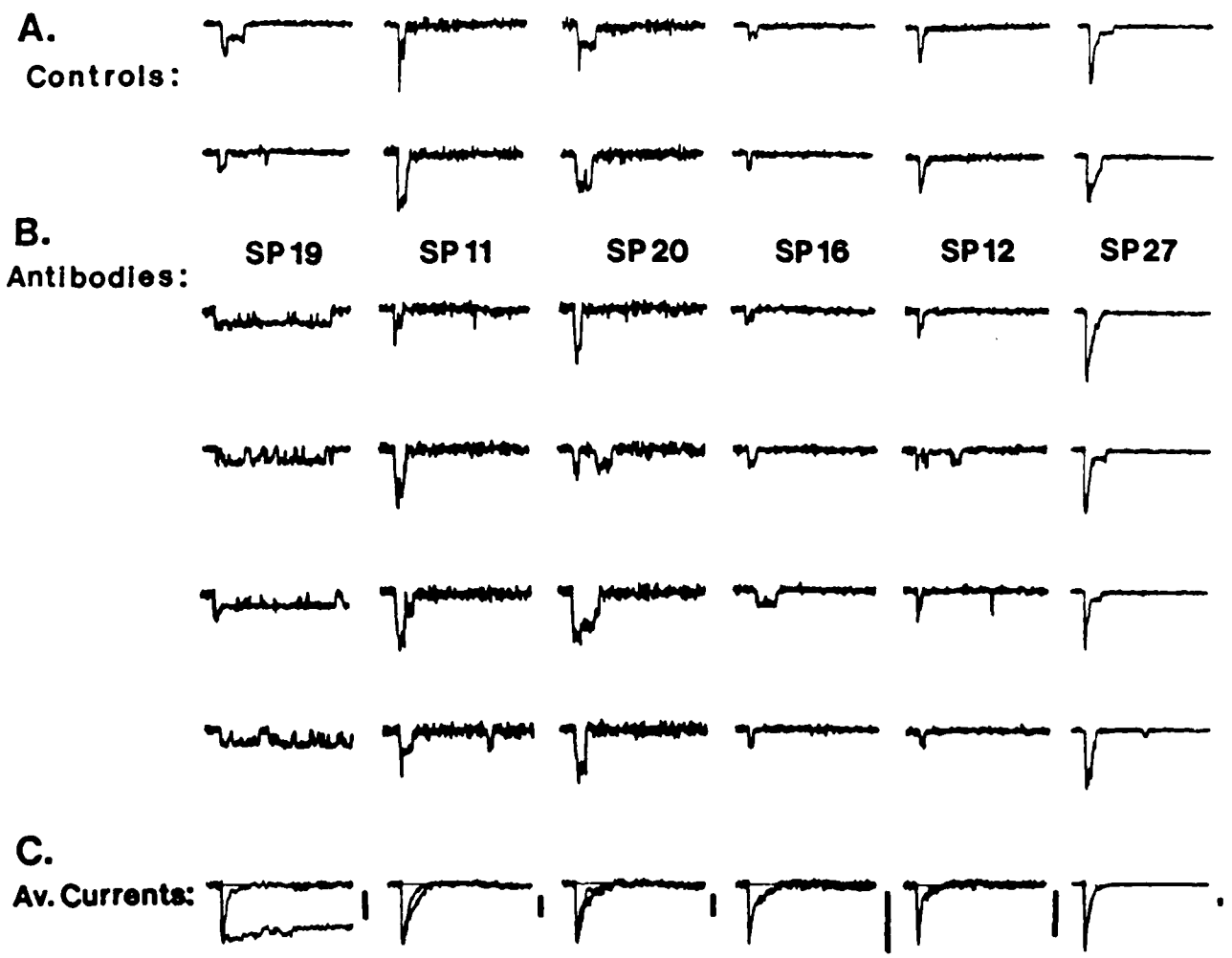

Figure 4. *Effects of site-directed antibodies on single sodium channel currents.* Depolarizing test pulses to -20 mV for 25 ms were applied from a holding potential of -140 mV. Pulses were delivered at a frequency of 1 Hz. Two representative current traces for each membrane patch under control conditions (panel A), four representative current traces in the presence of antibody (panel B), and superimposed average currents from 20 consecutive sweeps under control conditions and in the presence of antibody (panel C) are shown for each of the tested antibodies. The ensemble average currents in the presence of each of the antibodies were scaled and superimposed on the corresponding control currents to compare the time courses of inactivation in panel C.

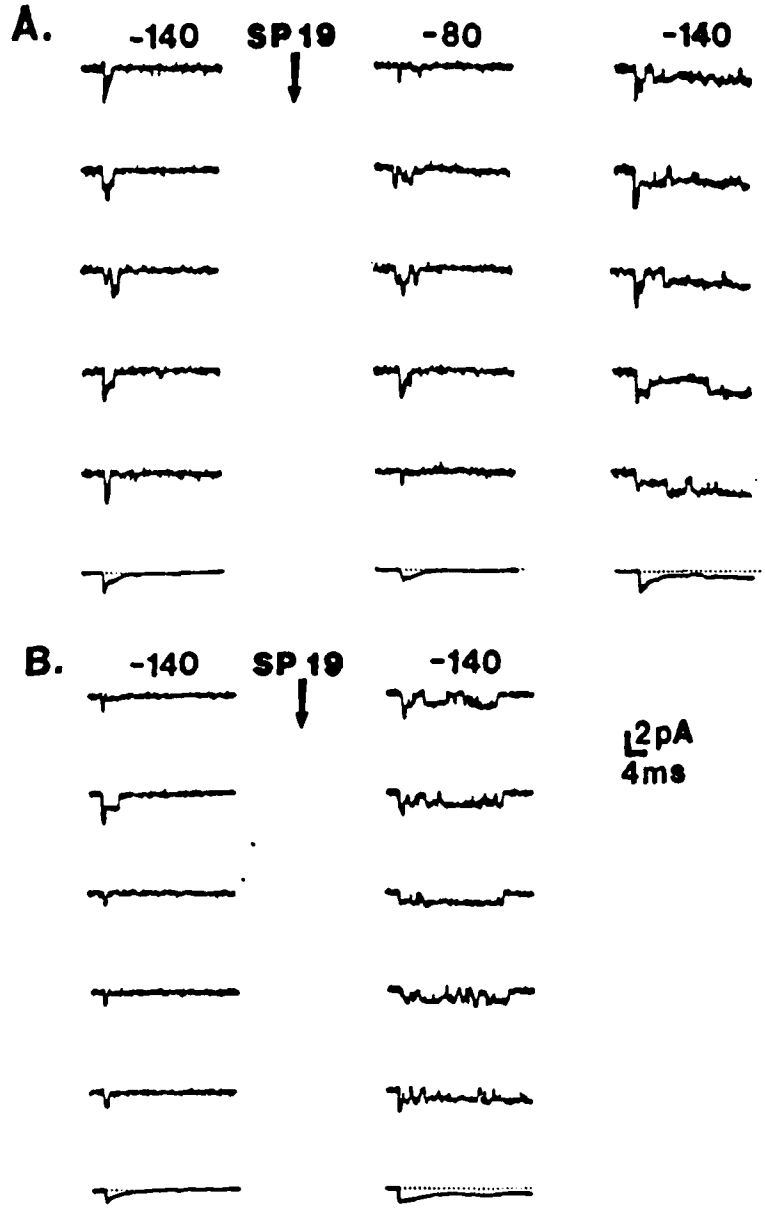

Figure 5. *Dependence of the rate of action of Ab_{SP19} on holding potential.* Sodium currents were stimulated by 25 ms test pulses to -10 mV. ***A. Left column.*** Control records were taken during a 15 min period at a holding potential of -140 mV. Five representative single channel traces and an average of 20 consecutive sweeps are presented. ***Middle column.*** The holding potential was changed to -70 mV and then to -80 mV. Ab_{SP19} was added to the cytoplasmic side of the membrane patch as indicated by the arrow, and the holding potential was maintained for an additional 6.5 min at -80 mV. Five single channel current traces and an average of 20 consecutive sweeps recorded between 6 and 6.5 min after adding Ab_{SP19} are shown. ***Right column.*** The holding potential then was changed to -140 mV. After 50 sec, five single channel traces and an average of 20 consecutive traces were recorded. ***B. Left column.*** In a different membrane patch, the membrane potential was held at -140 mV for 5 min in the absence of Ab_{SP19} and five single channel traces and an average of 20 consecutive sweeps were recorded. ***Right column.*** Ab_{SP19} was added as indicated by the arrow and 90 sec later five single channel traces and an average of 20 consecutive traces were recorded.

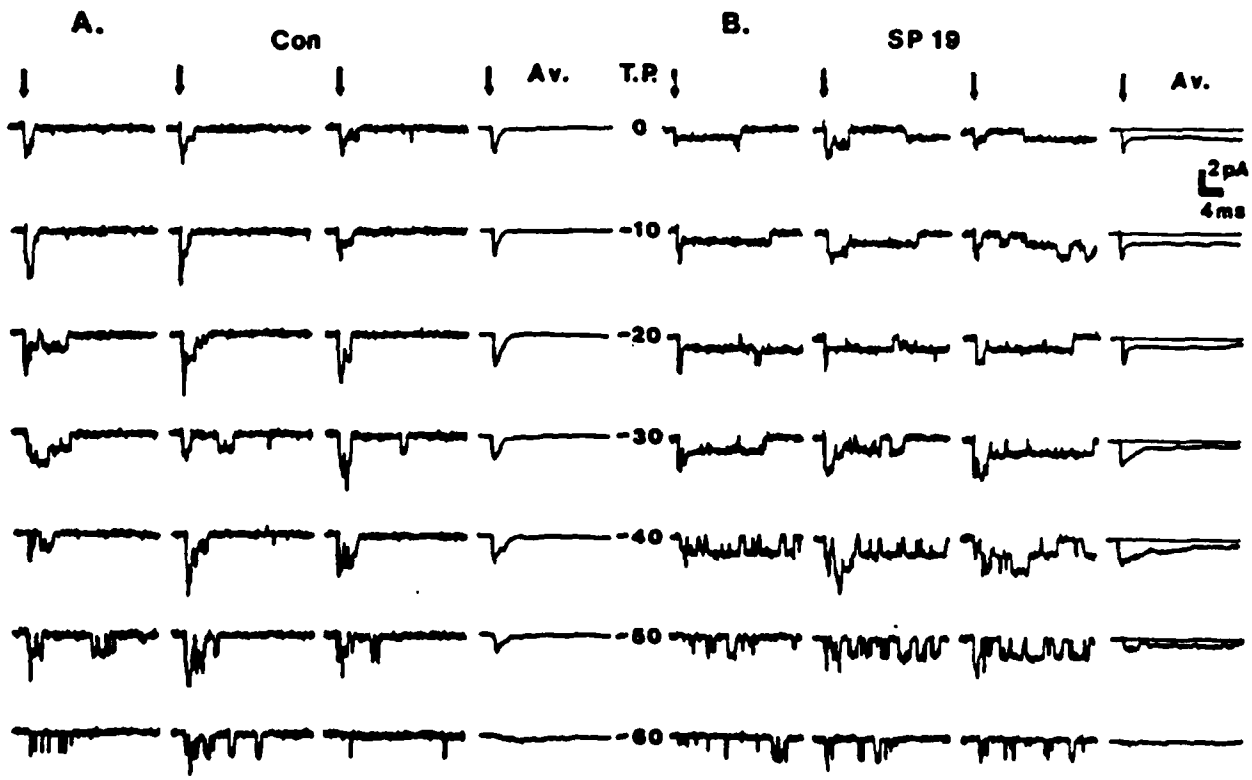

Figure 6. *Effect of Ab_{SP19} on single Na channel currents at different test potentials.* Sodium currents were elicited from a constant holding potential of -140 mV by 25 msec pulses to different test voltages as indicated. Three representative single channel sweeps and one ensemble average current trace (Av.) are shown for each test potential under control conditions ***(A)*** and in the presence of Ab_{SP19} ***(B)***. Arrows above the top current traces indicate the onset of the depolarizing pulses. In the panel showing the average currents in ***(B)***, the zero current levels have been marked with straight lines.

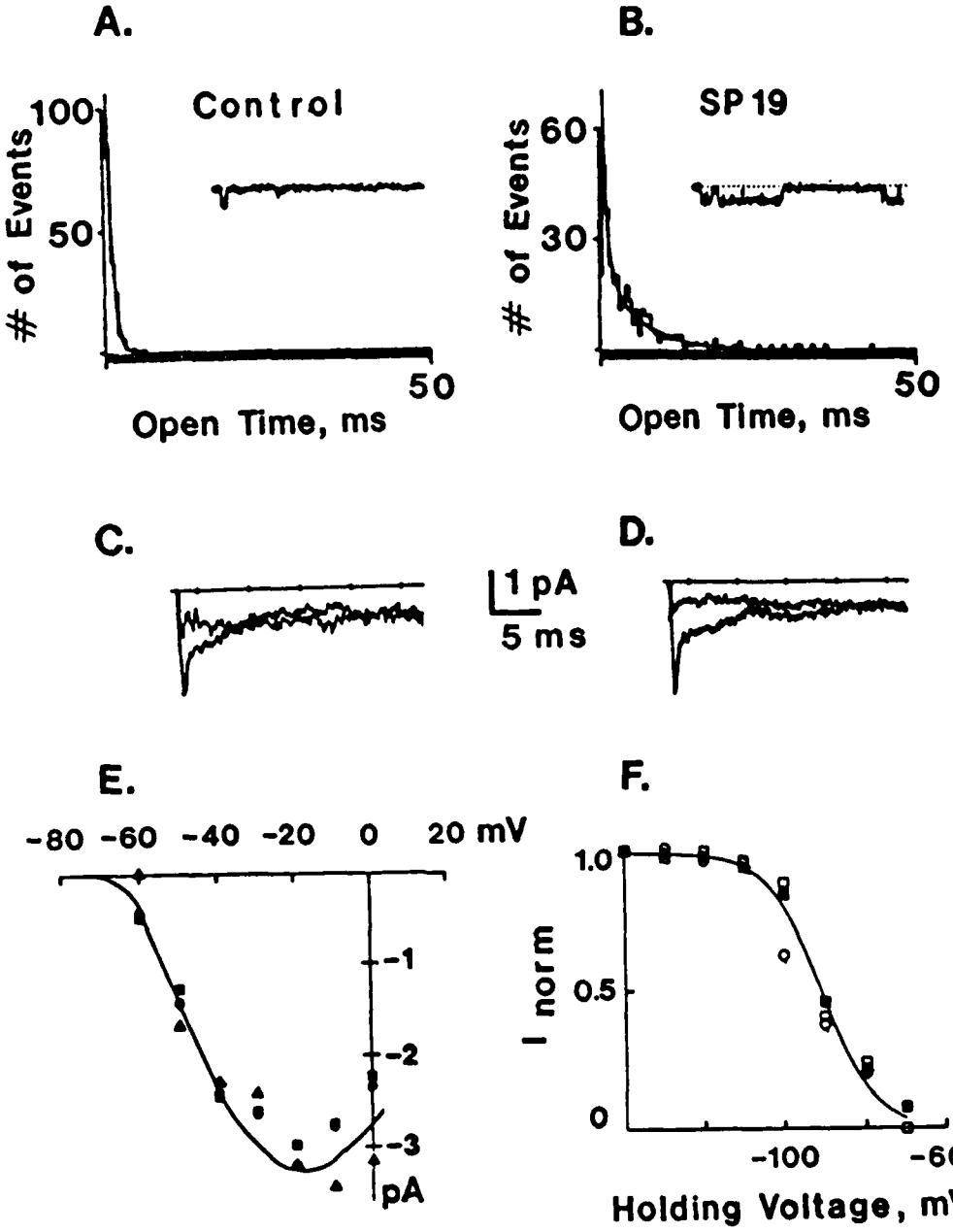
A.
Control
100
50
# of Events
50
Open Time, ms
B.
SP 19
60
30
# of Events
50
Open Time, ms
C.
1 pA
5 ms
D.
E.
-80 -60 -40 -20 0 20 mV
-1
-2
-3
pA
F.
1.0
0.5
0
I norm
-100
-60
Holding Voltage, mV

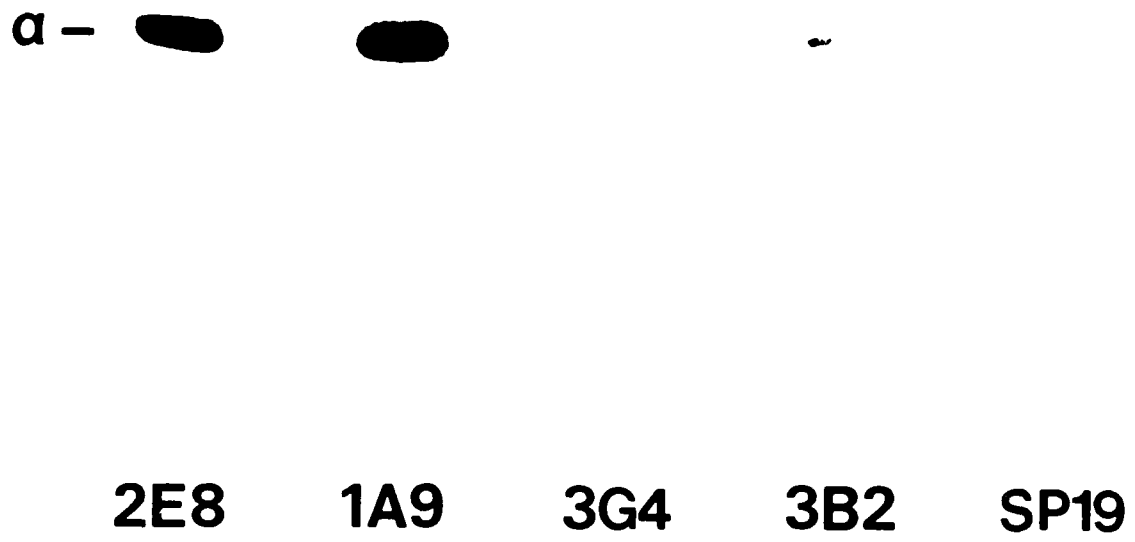

Figure 8. *Specific recognition of the α subunit by monoclonal antibodies against intact rat brain sodium channels.* Purified sodium channels were subjected to SDS-PAGE, transferred to Immobilon PVDF sheets, probed with antibody and ^{125}I-protein A, and subjected to autoradiography as described under Experimental Procedures. Recognition of the sodium channel α subunit by antisera raised against SP1491-1508 and migration of myosin, Mr 200,000 are shown for comparison. For 1G11, 3 pmol channel was used; for all others, 1 pmol was used. For 1A9 and anti-SP1491-1508, autoradiograms were exposed for 3 hr; all others were exposed for 48 hr.

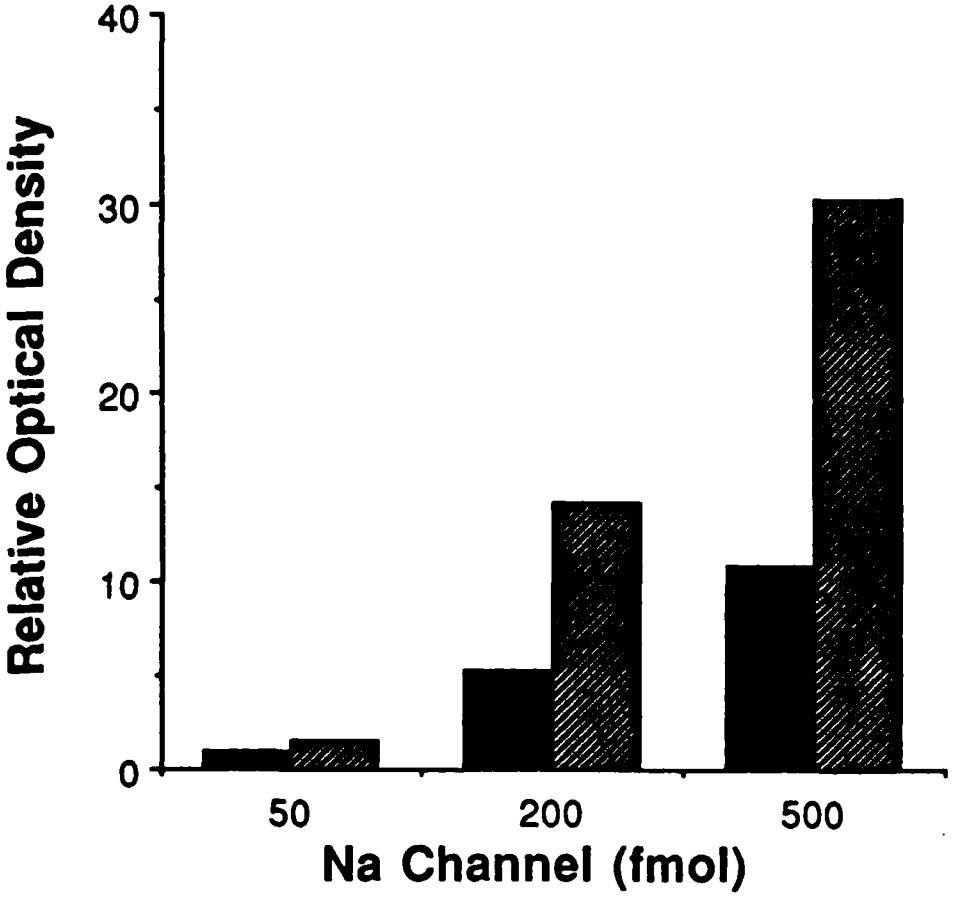

Figure 9. *Binding of monoclonal antibodies to denatured and nondenatured sodium channels.* Increasing amounts of untreated or SDS-denatured sodium channels bound to nitrocellulose were incubated with 2E8 at a dilution of 1/100, and bound antibody visualized by ^{125}I-Protein A binding and autoradiography. Bound ^{125}I was quantified by laser densitometry and all values were standardized relative to that for 50 fmol denatured sodium channels.

Figure 10. *Immunoprecipitation of sodium channels in the presence of synthetic peptides.* ^{32}P-labeled sodium channels were incubated with the indicated antibody in the presence or absence of the indicated peptides at 50 μM, and antibody-bound sodium channels were immunoprecipitated with protein A-Sepharose as described under Experimental Procedures. Percent block of immunoprecipitation by each peptide is plotted versus the amino acid sequence number of the N and C terminal residues of each peptide. Results were calculated as the percent block of immunoprecipitation by comparing the amount of ^{32}P-sodium channel bound in the presence and absence of peptide.

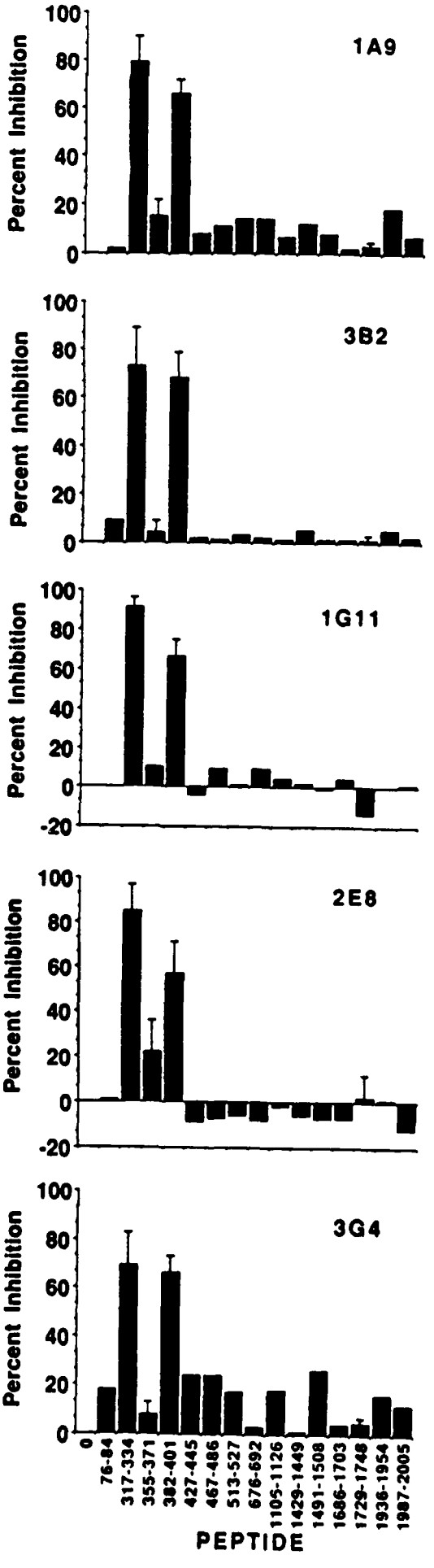
1A9
3B2
1G11
2E8
3G4
Percent Inhibition
100
80
60
40
20
0
-20
0
76-84
317-334
355-371
382-401
427-445
467-486
513-527
676-692
1105-1126
1429-1449
1491-1508
1686-1703
1729-1748
1936-1954
1987-2005
PEPTIDE

Figure 11. *Concentration dependence for block of immunoprecipitation of ^{32}P-labeled sodium channels by synthetic peptides or unlabeled sodium channels.* ^{32}P-labeled sodium channels were immunoprecipitated with the indicated antibody in the presence of increasing amounts of unlabeled sodium channel (▲), SP317-334 (■) or SP382-400 (●) as described under Experimental Procedures. Immunoprecipitation is expressed as a percent of the maximum value precipitated in the absence of unlabeled antigen.

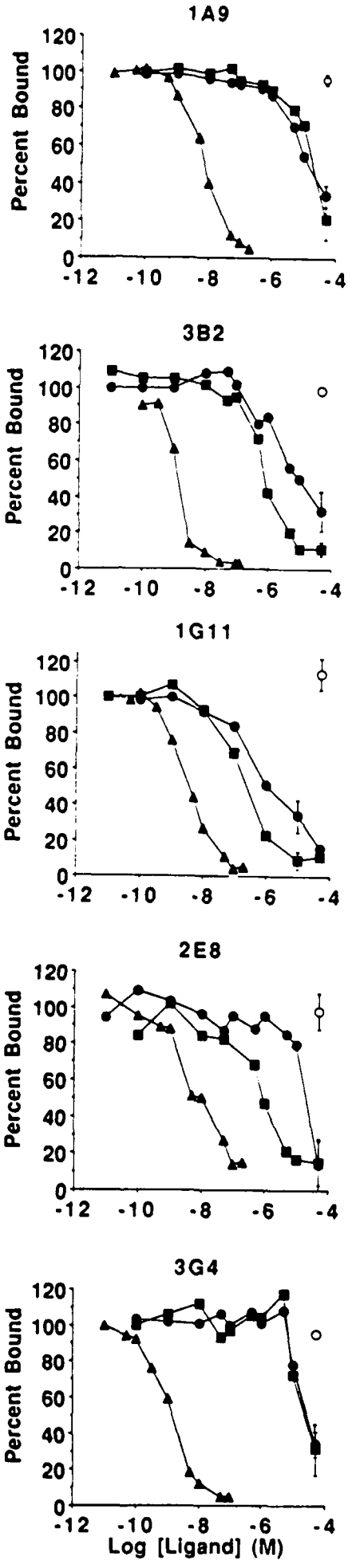
1A9
3B2
1G11
2E8
3G4
Percent Bound
120
100
80
60
40
20
0
-12
-10
-8
-6
-4
Log [Ligand] (M)

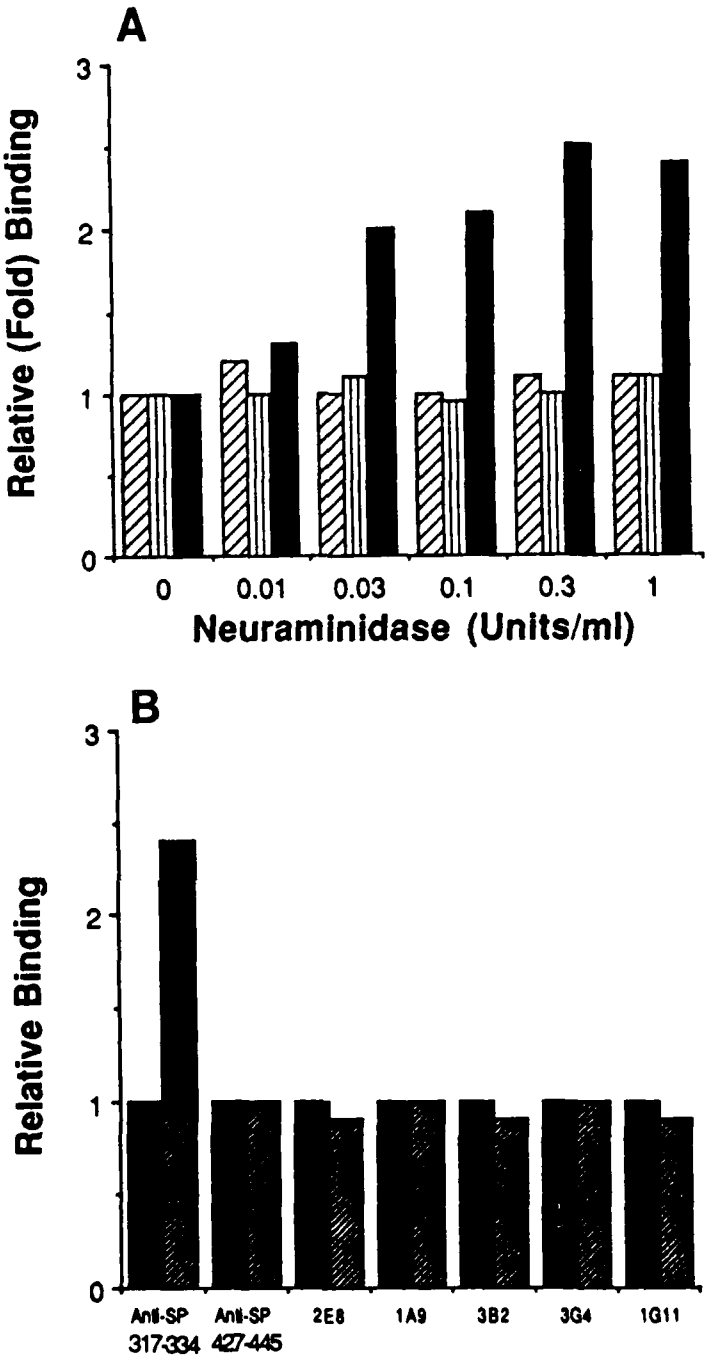

Figure 12. *Effect of deglycosylation on recognition of sodium channels by monoclonal antibodies or anti-peptide antibodies.* ^{32}P-labeled sodium channels were incubated for one hr on ice with or without neuraminidase. Antibody was added, the samples were mixed overnight, and antibody-bound sodium channels were precipitated with protein A-Sepharose. Results are expressed as the fraction of control untreated sodium channels that was immunoprecipitated by each antibody after neuraminidase treatment. *A)* Immunoprecipitation of ^{32}P-labeled sodium channels by 1G11(▨), anti-SP$_{317-334}$ (■), or anti-SP$_{427-445}$ (▥) after treatment with increasing concentrations of neuraminidase. *B)* Immunoprecipitation of control (■) or neuraminidase-treated (▨) ^{32}P-labeled sodium channels by monoclonal antibodies, anti-SP$_{317-334}$ or anti-SP$_{427-445}$. Neuraminidase was used at a concentration of 1 unit/ml.

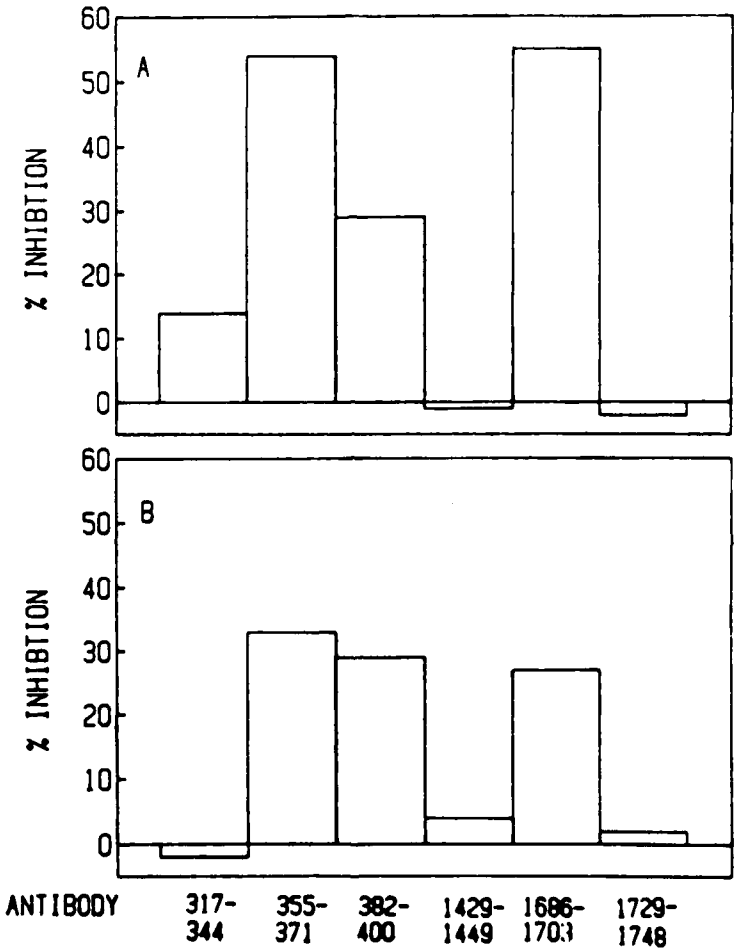

Figure 13. *Inhibition of ^{125}I-LqTx binding by site-directed antibodies.* ***(A)*** Sodium channels in reconstituted phospholipid vesicles were preincubated with 5.5 μM preimmune IgG or 5.5 μM of the indicated site-directed antibodies (IgG) in a total volume of 300 μl containing 50 mM NaCl, 3 mM Hepes-Tris, 133 mM glycine HCl, pH 7.4, and 1 μM BTx for four hours at 4°C with rotation, and ^{125}I-LqTx binding was measured as described under Experimental Procedures. ***(B)*** Rat brain synaptosomes (50 μl of a 25 mg/ml suspension) were preincubated with 5.5 μM preimmune IgG or 5.5 μM of the indicated site-directed antibodies, in a total volume of 300 μl of 25 mM NaCl, 2 mM Hepes-Tris, 133 mM glycine HCl, pH 7.4, and 1 μM BTx, and ^{125}I-LqTx binding was measured as described under Experimental Procedures. In both panels A and B, the data are expressed as the percentage inhibition as compared to control samples having only preimmune IgG.

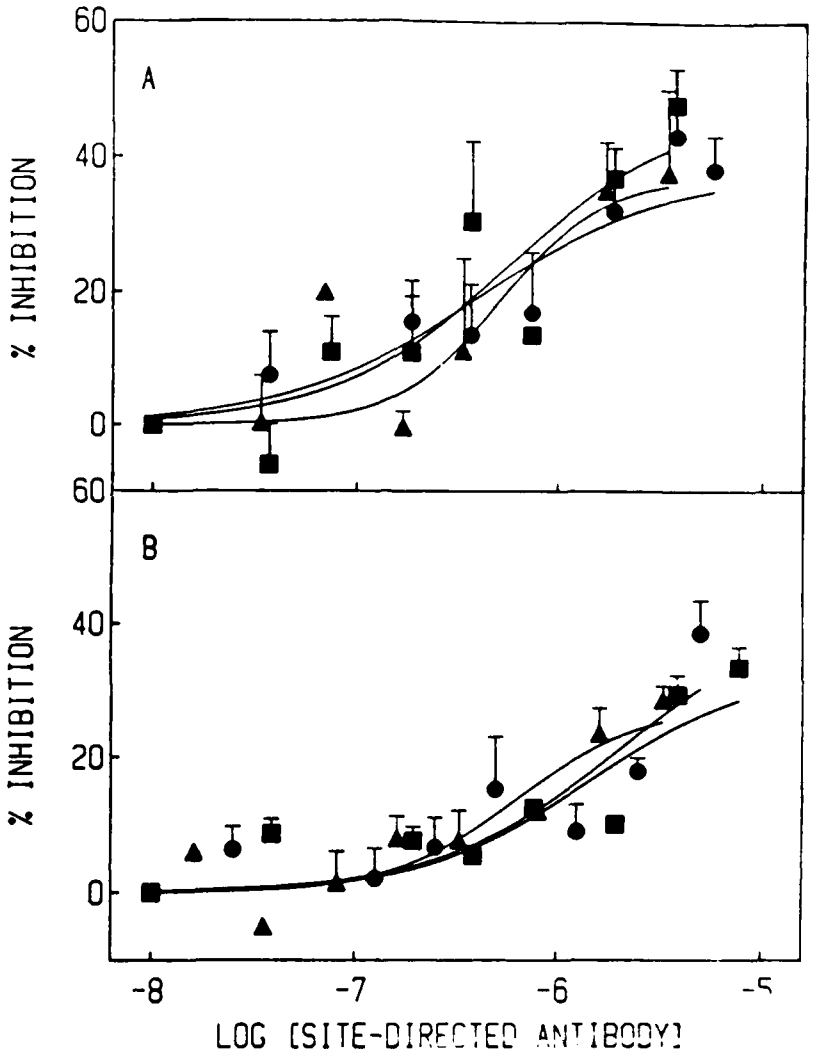

Figure 14. *Concentration- dependence of the inhibition of ^{125}I-LqTx binding site-directed antibodies.* ***(A)*** Inhibition of ^{125}I-LqTx binding to sodium channels reconstituted in phospholipid vesicles by $Ab_{382-400}$ (circles), $Ab_{1686-1703}$ (squares), and $Ab_{355-371}$ (triangles). Sodium channels in reconstituted phospholipid vesicles (100 µl) were preincubated for four hours with the indicated concentrations of site-directed antibodies, 2 µM preimmune IgG, and 1 µM BTx, in a total volume of 300 µl containing 50 mM NaCl, 3 mM Hepes-Tris, 133 mM glycine HCl, pH 7.4, and 1 µM BTx with rotation, and ^{125}I-LqTx binding was measured as described under Experimental Procedures.. The percentage inhibition at each antibody concentration was calculated from controls that contained only preimmune IgG. Each data point represents the mean +/- SEM of three to five independent experiments where triplicate determinations were made at each antibody concentraion. Curves represent fits of data to a sigmoidal function by a nonlinear-least squares curve fitting program (Graph Pad, ICI). ***(B)*** Inhibition of ^{125}I-LqTx binding to rat brain synaptosomes by $Ab_{382-400}$ (circles), $Ab_{1686-1703}$ (squares), and $Ab_{355-371}$ (triangles). Synaptosomes (50 µl of 25 mg/ml) were preincubated with 7 µM preimmune IgG and the indicated concentrations of site-directed antibodies in a total volume of 300 µl of 25 mM NaCl, 2 mM Hepes-Tris, 133 mM glycine HCl, pH 7.4, and 1 µM BTx, and ^{125}I-LqTx binding was measured as described under Experimental Procedures. Each data point represents the mean +/- SEM of three to four separate experiments in which triplicate determinations were made at each antibody concentration. Data were fit as described in panel A.

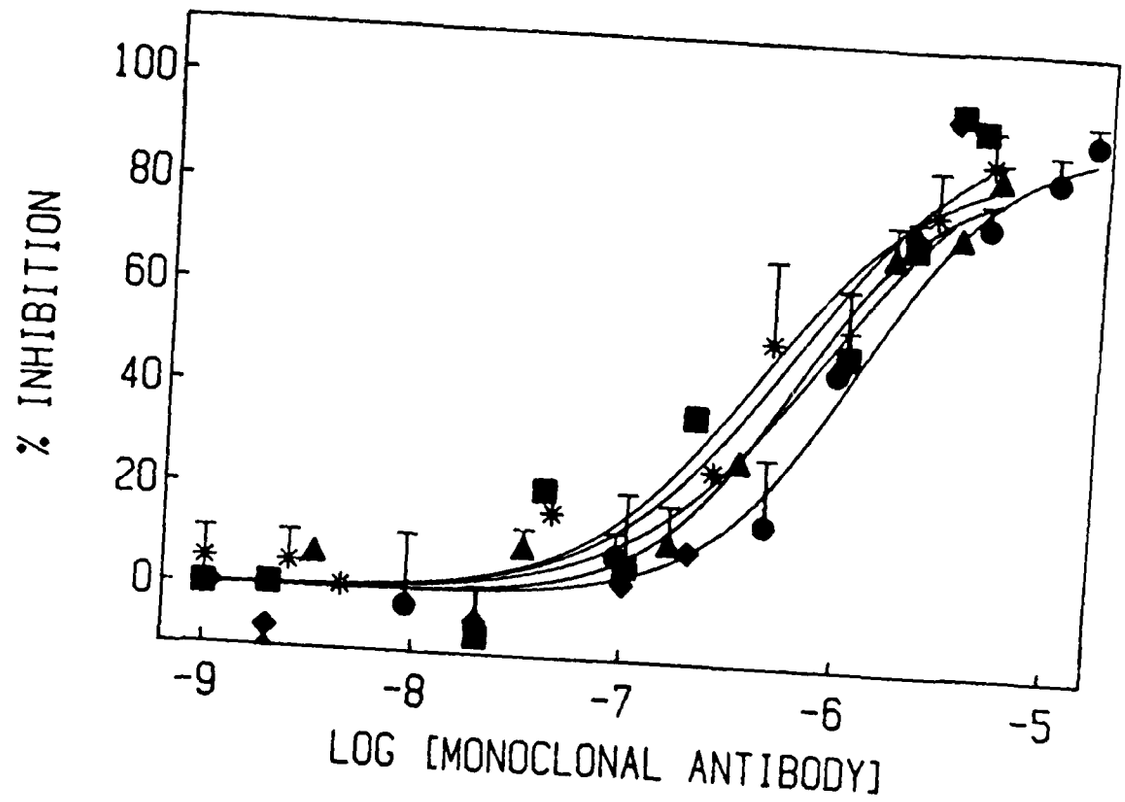

Figure 15. *Concentration-dependence of monoclonal antibody-mediated inhibition of ^{125}I-LqTx binding to synaptosomes. (A)* Inhibition of ^{125}I-LqTx binding to rat brain synaptosomes by monoclonal antibodies 1G11 (circles), 1A9 (squares), 2E8 (triangles), 3B2 (diamonds), and 3G4 (asterisk). Synaptosomes (50 µl of 25 mg/ml) were preincubated for four hours at 4°C with rotation with 7 µM preimmune IgG and the indicated concentrations of monoclonal antibodies in a total volume of 300 µl of 25 mM NaCl, 2 mM Hepes-Tris, 133 mM glycine HCl, pH 7.4, and 1 µM BTx, and ^{125}I-LqTx binding was measured as described under Experimental Procedures. Each data point is expressed as percent inhibition calculated from controls in which no antibody was added. Each point represents the mean +/- SEM of two separate experiments in which triplicates were done at each antibody concentration. Data were analyzed as described in Figure 2.

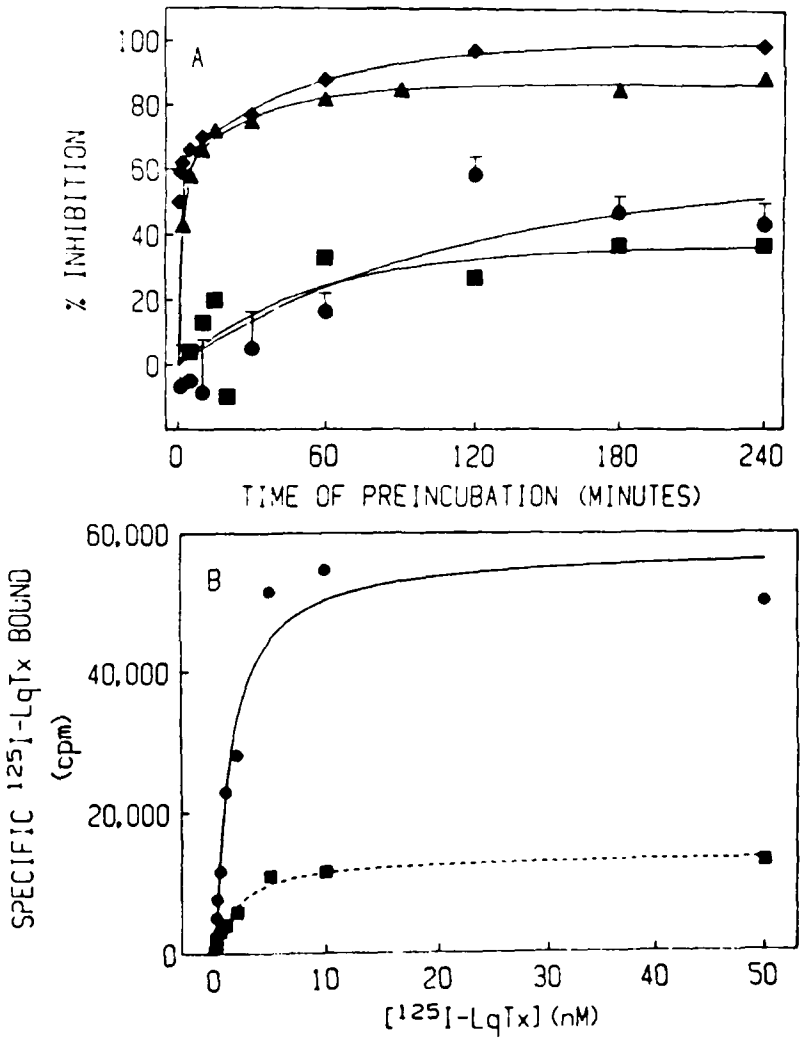

Figure 16. *Time course and saturation isotherm for inhibition of ^{125}I-LqTx binding. (A) Ab382-400.* Rat brain synaptosomes were preincubated with 1 μM $Ab_{382-400}$ and 2 μM preimmune IgG *(squares)* in 25 mM NaCl, 2 mM Hepes-Tris, 130 mM glycine HCl, pH 7.4, and 1 μM BTx at 4°C. Sodium channels in reconstituted phospholipid vesicles were preincubated with 1 μM $Ab_{382-400}$ *(circles)* and 2 mM preimmune IgG in 17 mM NaCl, 1mM Hepes-Tris, 130 mM glycine HCl, pH 7.4, and 1 μM BTx at 4°C. At the indicated times, aliquots were removed and binding of ^{125}I-LqTx was measured as described under Experimental Procedures. *mAb 3G4.* Rat brain synaptosomes *(diamonds)* or sodium channels in reconstituted vesicles *(triangles)* were preincubated with 6 μM mAb 3G4 in 15 mM NaCl, 1 mM Hepes-Tris, 67 mM sodium citrate, pH 7.4. At the indicated times, aliquots were removed and binding of ^{125}I-LqTx was measured as described under Experimental Procedures. Data are expressed as percentage inhibition based on controls obtained at each time point. Each data point represents the mean +/- SEM of three experiments for reconstituted vesicles studied with $Ab_{382-400}$ and one experiment for the other data. Triplicate determinations were made at each time point. Curves represent fits of data to a monoexponential function by a nonlinear least-squares curve fitting program (Graph Pad, ISI). ***(B)*** Rat brain synaptosomes were incubated with 0.01 to 50 nM ^{125}I-LqTx in the absence *(circles)* or presence *(squares)* of 1 μM mAb 1A9 in 15 mM NaCl, 1 mM Hepes-Tris, 67 mM sodium citrate , pH 7.4 and ^{125}I-LqTx binding was measures as described under Experimental Procedures. Points represent data from a single experiment in which triplicate determinations were made at each toxin concentration. Curves represent a nonlinear least-squares curve fit of data to a hyperbolic function (Graph Pad, ISI) which provided estimates of K_d and B_{max}.

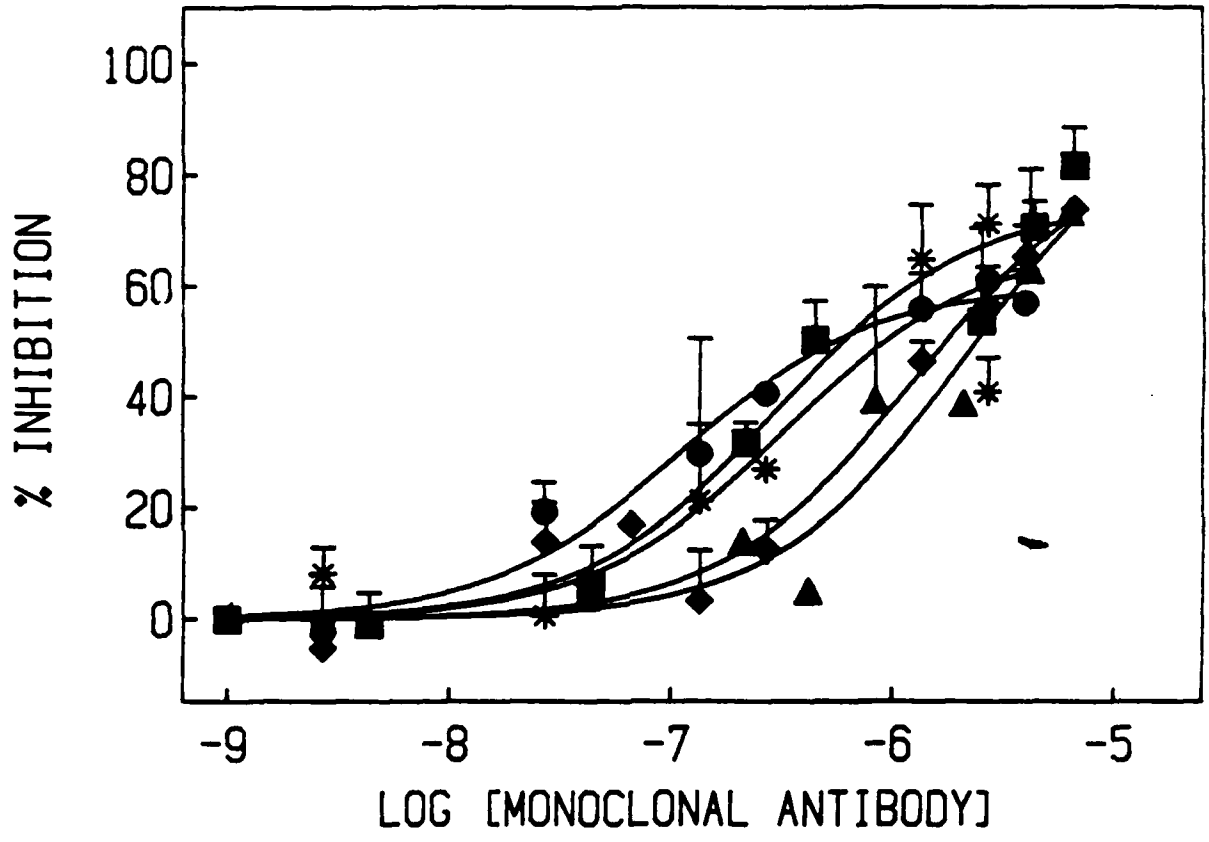

Figure 17. *Concentration-dependence of mAb-mediated inhibition of 125I-LqTx binding.* Inhibition of ^{125}I-LqTx binding to rat brain sodium channel reconstituted into phospholipid vesicles by mAbs 1G11 (●), 1A9 (■), 2E8 (▲), 3B2 (◆), (100 µl) were preincubated for 4 hrs at 4°C with rotation along with indicated concentrations of mAb (1-100 µl additions in 0.1 M citrate pH 7.4), 5.5 µM preimmune IgG (100 µl in 0.1M citrate, pH 7.4), and the volume was brought to a total of 300 µl with buffer containing 10 mM Hepes-Tris and 150 mM NaCl, pH 7.4. ^{125}I-LqTx was measured as described in Materials and Methods. Each data point is expressed as percent inhibition calculated from controls in which no antibody was added. Each point represents the mean ± SEM of four separate experiments (except 2E8, n = 2) in which triplicates were done at each antibody concentration. Curves represent fits of data to a sigmoidal function by a nonlinear least-squares curve-fitting program (Graph Pad, ISI).

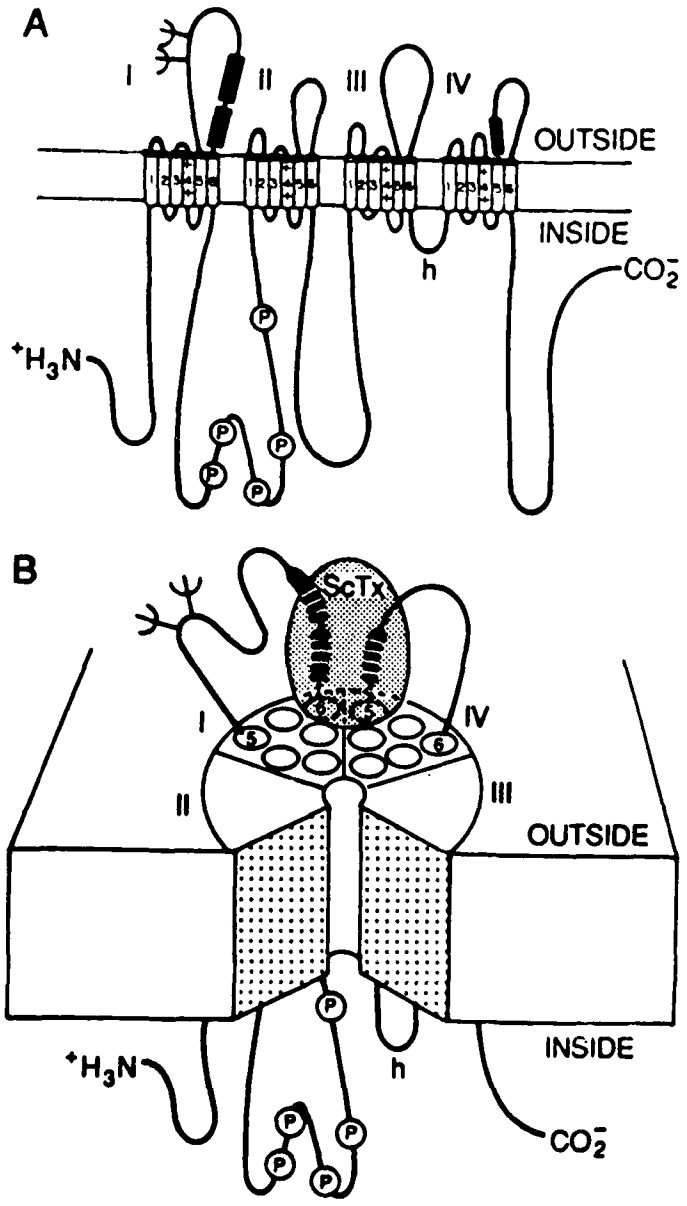

Figure 18. *Structure of the of the RII sodium channel α-subunit . (A)* A two-dimensional view of the proposed transmembrane folding of the sodium channel α subunit depicting the sites of interaction of the site-directed antibodies ($Ab_{355-371}$, $Ab_{382-400}$, and $Ab_{1676-1703}$) which inhibit LqTx binding (dark boxes), known sites of protein phosphorylation (P) and glycosylation (Ψ), and site of inactivation gating (h). ***(B)*** A three-dimensional view of the sodium channel α subunit showing the proposed folding of the four homologous domains which brings domains I and IV into close apposition and allows formation of a transmembrane pore . An α-scorpion toxin molecule (ScTx) is depicted binding to the channel by interaction with the extracellular sequences between transmembrane segments S5 and S6 of domains I and IV that are recognized by $Ab_{355-371}$, $Ab_{382-400}$, and $Ab_{1676-1703}$.

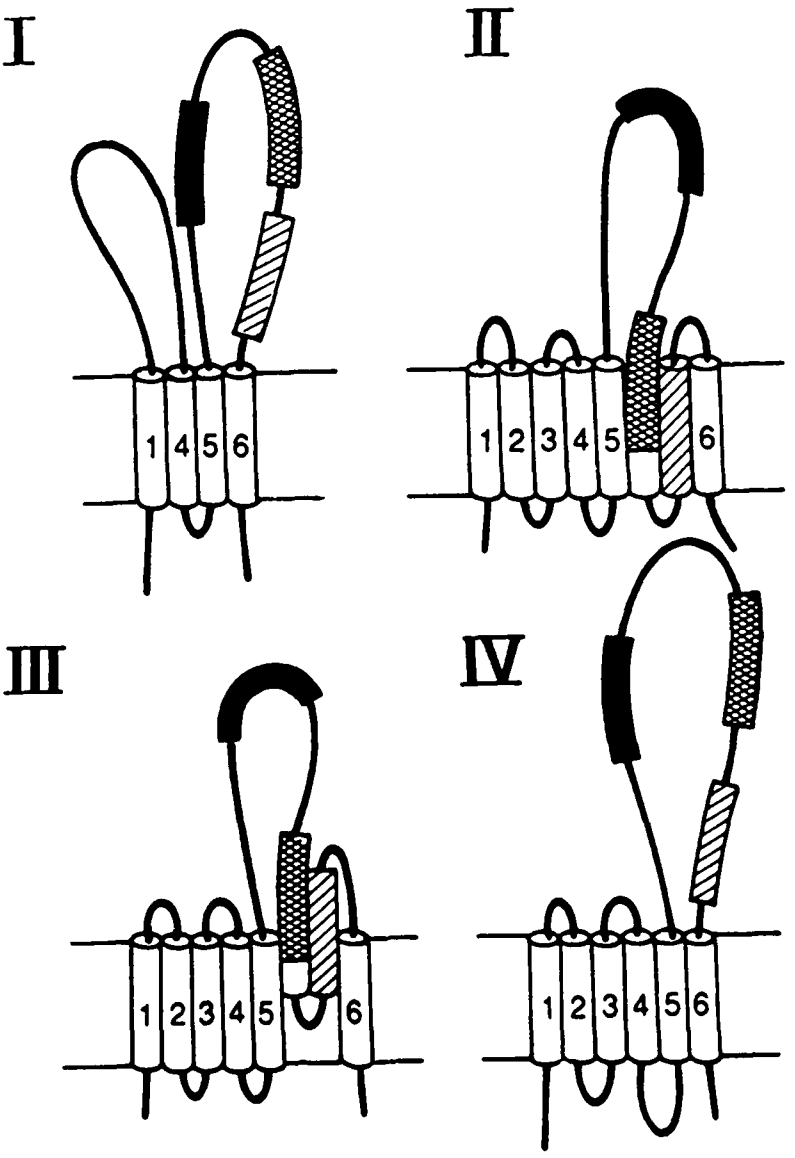

Figure 19. *Transmembrane folding models of domain I of the sodium channel α subunit.* Transmembrane folding models are presented as described in previous studies: 1, reference 12; model 2, reference 13; model 3, reference 14; model 4, references 5, 15.

REFERENCES

Aldrich, R. W., Corey, D. P. & Stevens, C. F. (1983) *Nature (Lond.)* **306,** 435-441.

Armstrong, C. M. (1981) *Physiological Reviews* **61**, 644-683.

Auld, V.J., Goldin, A.L., Krafte, D.S., Marshall, J., Dunn, J.M., Catterall, W.A., Lester, H.A., Davidson, N., and Dunn, R.J. (1988) *Neuron* **1,** 449-461.

Beneski, D. A., & Catterall, W. A. (1981) *Proc. Nat. Acad. Sci. USA* **77,** 639-642.

Benjamin, D.C., Berzofsky, J.A., East, I.J., Gurd, F.K.N., Hannum, C., Leach, S.J., Margoliash, E., Michael, J.G., Miller, A., Prager, E.M., Reichlin, M., Sercaz, E.E., Smith-Gill, S.J., Todd, P.E., and Wilson, A.C. (1984) *Ann. Rev. Immunol.* **2,** 67-101..

Catterall, W. A. (1976) *J. Biol. Chem.* **251,** 5528-5536.

Catterall, W. A. (1986) *Ann. Rev. Biochem.* **55,** 953.-985

Catterall, W. A., Morrow, C. S., and Hartshorne, R. P. (1979)*J. Biol. Chem.* **254,** 11379-11387.

Catterall, W.A. (1977) *J. Biol. Chem.* **252,** 8660-8668.

Catterall, W.A. (1979) *J. Gen. Physiol.* **74,** 375-391.

Catterall, W.A. (1986) *Annu. Rev. Biochem.* **55,** 953-985.

Catterall, W.A. (1988a) *ISI Atlas of Science: Pharmacol.* 190-195.

Catterall, W.A. (1988b) *Science* **242,** 50-61.

Coombs, J., *et al.* (1988) *Biophys.J.* **53,** 542a .

Costa, M.R.C., and Catterall, W.A. (1984) *J. Biol. Chem.* **259,** 8210-8218.

Ellis, L. *et al.* (1986)*Cell* **45,** 721.

Feller, D.J., Talvenheimo, J.A. & Catterall, W.A. (1985a) *J. Biol. Chem.* **260,** 11542-11547.

Feller, D.J., Talvenheimo, J.A., and Catterall, W.A. (1985b) *J. Biol. Chem.* **262,** 17530-17535.

Fontecilla-Camps, J.C., Habersetzer-Rochat, C. & Rochat, H. (1988) *Proc. Natl. Acad. Sci. USA* **85,** 7443-7447.

Glisin, V. , Crkvenjakov, R., and Byus, C. (1973)*Biochemistry* **13**, 2633.

Goding, J.W. (1978) *J. Immunol. Meth.* **20,** 241-253.

Goding, J.W. (1983) *Monoclonal Antibodies: Principals and Practice*, pp. 56-97, Academic Press, New York.

Goldin, A. L. *et al.* (1988)*Soc. Neurosci. Abs.* **14,** 598.

Goldin, A.L. Snutch, T., Lubbert, H., Dowsett, A., Marshall, J., Auld, V., Downey, W., Fritz, L., Lester, H., Dunn, R., Catterall, W.A., and Davidson, N. (1986) *Proc. Natl. Acad. Sci. USA* **83,** 7503-7507.

Gonoi, T. & Hille, B. (1987) *J. Gen. Physiol.* **89,** 253-274.

Gonoi, T., Hille, B., and Catterall, W. A. (1984) *J. Neurosci.* **4,** 2836.

Gordon, D. A., Merrick, D., Wollner, D.A., & Catterall, W.A. (1988) *Biochemistry* **27,** 7032-7038.

Gordon, D., Merrick, D., Auld, V., Dunn, R., Goldin A. L., Davidson, N. & Catterall, W. A. (1987) *Proc. Natl. Acad. Sci. USA* **84,** 8682-8686.

Gordon, R.D., Fieles, W.E., Schotland, D.L., Angeletti, R.A. & Barchi, R.L. (1987) *Proc. Natl. Acad. Sci. USA* **84,** 308-313.

Gordon, R.D., Li, Y., Fieles, W.E., Schotland, D.L. & Barchi, R.L. (1988) *Neuroscience* **8,** 3742-3749.

Gordon, R.D., Li, Y., Fieles, W.E., Schotland, D.L., and Barchi, R.L. (1988) *J. Neurosci.* **8,** 3742-3749.

Greenblatt, R.E., Blatt, Y. & Montal, M. (1985) *FEBS Lett.* **193,** 125-134.

Guy, H.R. & Seetharamulu, P. (1986) *Proc. Natl. Acad. Sci. USA* **83,** 508-512.

Hamill, O., Marty, A., Neher, E., Sakmann, B. & Sigworth, F. J. (1981) *Pfluegers Arch.* **391,** 85-100.

Hartshorne, R.P., and Catterall, W.A. (1984) *J. Biol. Chem.* **259,** 1667-1675.

Hille, B. (1984) *Ionic Channels in Excitable Membranes* (Sinauer, Sunderland, MA).

Horn, R. & Vandenberg, C. A. (1984) *J. Gen. Physiol.* **84,** 505-534.

Huguenard, J., Hamill, O. P., and Prince, D. A. (1988) *J. Neurophysiol.* **59,** 778.

Jover, E., Massacrier, A., Cau, P., Martin, M.-F. & Couraud, F. (1988) *J. Biol. Chem.* **263,** 1542-1548.

Kanner, B.I. (1978) *Biochemistry* **17,** 1207-1211.

Kayano, T., Noda, M., Flockerzi, V., Takahashi, H., & Numa, S. (1988) *FEBS Lett.* **228,** 187-194.

Kirsch, G. E., Skattebol, A. , Possani, L., and Brown, A.M. (1989) *J. Gen. Physiol.* **93,** 67.

Kopenhofer, E., and Schmidt, H. (1968) *Pflüger's Arch.* **303,** 133.

Kosower, E.M. (1985) *FEBS Lett.* **182,** 234-242.

Kraner, S.D., Tanaka, J.C., and Barchi, R.L. (1985) *J. Biol. Chem.* **260,** 6341-6347.

Leibowitz, M. D., Sutro, J. B., and Hille, B. (1986) *J. Gen. Physiol.* **87,** 25.

Maizel, J.V. (1987) *J. Biol. Chem.* **262,** 10035-10038.

Matsudaira, P. (1987) *J. Biol. Chem.* **262,** 10035-10038.

Melton, D. A., Kreig, P. A., Rebaliati, M. R., and Maniatis, T. (1984) *Nucleic Acid Res.* **12,** 7035.

Meves, H., Simard, J.M. & Watt, D.D. (1986) *Ann. N.Y. Acad. Sci.* **479,** 113-132.

Miller, J.A., Agnew, W.S., and Levinson, S.R. (1983) *Biochemistry* **22,** 462-470.

Moolenaar, W. H, and Spector, I. (1978) *J. Physiol.* **278,** 265.

Moorman, J. R., Kirsch, G. E., and Brown, A. M. (1989) *Biophys. J.* **55,** 229a.

Noda, M., Ikeda, T., Kayano, T., Suzuki, H., Takeshima, H., Kurasaki, M., Takahashi, H. & Numa, S. (1986a) *Nature (Lond.)* **320,** 188-192.

Noda, M., Ikeda, T., Kayano, T., Suzuki, H., Takashima, H., Kuno, M. & Numa, S. (1986b) *Nature (Lond.)* **322,** 826-828.

Noda, M., Shimizu, S., Tanabe, T., Takai, T., Kayano, T., Ikeda, T., Takahashi, H., Nakayama, H., Kanaoka, Y., Minamino, N., Kangawa, K., Matsuo, H., Raftery, M., Hirose, T., Inayama, S., Hayashida, H., Miyata, T., and Numa, S. (1984) *Nature* **312,** 121-127.

Rando, T. A., Wang, G. K., and Strichartz, G. R. (1986)*J. Pharmacol. Exp. Ther.* **29,** 467.

Rando, T. A., Wang, G. K., Strichartz, G. R. (1989)*J. Gen. Physiol.* **93,** 43.

Rasmussen, C. D., Simmen, R. C. M., MacDougall, E. A., and Means, A. R. (1987) *Meth. Enzymol.* **139,** 642.

Rossie, S., and Catterall, W.A. (1987) *J. Biol. Chem.* **262,** 12735-12744.

Rossie, S., and Catterall, W.A. (1989) *J. Biol. Chem.* **264,** 14220-14224.

Rossie, S., Gordon, D. & Catterall, W.A. (1987) *J. Biol. Chem.* **262,** 17530-17535.

Sah, P., Gibb, A. J., and Gage, P. W. (1988) *J. Gen. Physiol.* **91,** 373.

Salgado, V. L., Yeh, J. Z., & Narahashi, T. (1985) *Biophys. J.* **47**, 567-571.

Scheuer, T., Boyd, S., Auld, V. J., Dunn R. J., & Catterall, W. A. (1989) *Biophys. J.* **55,** 318a.

Sharkey, R.G., Beneski, D.A. & Catterall, W. A. (1984) *Biochemistry* **23,** 6078-6086.

Stafstrom, C. E., *et al.* (1985)*J . Neurophysiol.* **53,** 153.

Strichartz, G., Rando, T. & Wang, G.K. (1987) *Annu. Rev. Neurosci.* **10,** 237-267.

Stühmer W., *et al.* (1987) *Eur. Biophys. J.* **14,** 131.

Stühmer, W., Conti, F., Suzuki, H., Wang, X., Noda, M., Yahagi, N., Kubo, H. & Numa, S. (1989) *Nature (Lond.)* **339,** 597-603.

Sutro, J. B. (1986) *J. Gen. Physiol.* **87,** 1.

Suzuki, H., Beckh, S., Kubo, H., Yahagi, N., Ishida, H., Kayano, T., Noda, M., & Numa, S. (1988) *FEBS Lett.* **228**, 195-200.

Talvenheimo, J.A., Tamkun, M.M., and Catterall, W.A. (1982) *J. Biol. Chem.* **257,** 11868-11871.

Tamkun, M.M., Talvenheimo, J.A., and Catterall, W.A. (1984) *J. Biol. Chem.* **259,** 1676-1688.

Tejedor, F.J., and Catterall, W.A. (1989) *Proc. Natl. Acad. Sci. USA* **85,** 8742-8746.

Thomsen, W.J., and Catterall, W.A. (1989) *Proc. Natl. Acad. Sci. USA* **86,** in press

Trimmer, J.S., Cooperman, S.S., Tomika, S.A., Zhou, J., Crean, S.M., Boyle, M.B., Kallen, R.G., Shena, Z., Barchi, R.L., Sigworth, F.J., Goodman, R.H., Agnew, W.S., and Mandell, G. (1989) *Neuron* **3,** 33-49.

Tzartos, S., and Lindstrom, J. (1980) *Proc. Natl. Acad. Sci. USA* **77,** 755-759.

Ulbricht, W. (1969) *Ergebnisse der Physiologie* **61,** 18.

Vassilev, P., Scheuer, T. & Catterall, W.A. (1988) *Science* **241,** 1658-1661.

Vassilev, P., Scheuer, T., and Catterall, W. A. (1989) *Proc. Nat. Acad. Sci. USA*, in press.

Wang, G. K., and Strichartz, G. (1985) *J. Gen. Physiol.* **86,** 739 .

Yue, D. T., Lawrence, J. H. & Marban, E. (1989) *Science* **44,** 349-352.

DISTRIBUTION LIST

4 copies	Commander U.S. Army Medical Research Institute of Infectious Diseases ATTN: SGRD-UIZ-M Fort Detrick, Frederick, MD 21701-5011
1 copy	Commander U.S. Army Medical Research and Development Center ATTN: SGRD-RMI-S Fort Detrick, Frederick, MD 21701-5012
2 copies	Defense Technical Information Center (DTIC) ATTN: DTIC-DDAC Cameron Station Alexandria, VA 22304-6145
1 copy	Dean School of Medicine Uniformed Services University of the Health Sciences 4301 Jones Bridge Road Bethesda, MD 20814-4799
1 copy	Commandant Academy of Health Sciences, U.S. Army ATTN: AHS-CDM Fort Sam Houston, TX 78234-6100